

PARAMETRIC STUDIES OF WELDING OF 1.5% Mn FORGED STEEL PLATES

A DISSERTATION

*submitted in partial fulfilment of the
requirements for the award of the degree*

of

MASTER OF ENGINEERING

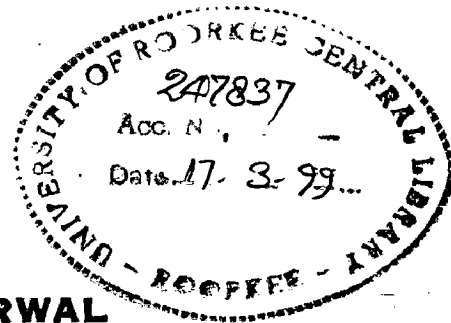
in

MECHANICAL ENGINEERING

(With Specialization in Welding Engineering)

By

V. K. AGARWAL



DEPARTMENT OF MECHANICAL & INDUSTRIAL ENGINEERING
UNIVERSITY OF ROORKEE
ROORKEE - 247 667 (INDIA)

OCTOBER, 1997

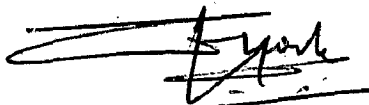
CANDIDATE'S DECLARATION

I hereby declare that the work, which is being presented in the dissertation entitled 'Parametric studies of Welding of 1.5% Mn forged steel plates' in partial fulfillment of the requirements for the award of the degree of **MASTER OF ENGINEERING (Welding Engineering)**, submitted in the Department of Mechanical and Industrial Engineering, **University of Roorkee**, Roorkee, is an authentic record of my own work carried out over a period of six months from April'97 to September'97, under the supervision of Dr. P.K. Ghosh, Scientist (Professor), Welding Research Laboratory, Department of Mechanical and Industrial Engineering. The matter embodied in this dissertation has not been submitted for the award of any other degree.

Dated : October 3rd, 1997


(V.K. AGARWAL)

This is to certify that the above statement made by the candidate is correct to the best of my knowledge.



(Dr. P.K. GHOSH)

Scientist (Professor)

Welding Research Laboratory Department of Mechanical & Industrial
Engineering

University of Roorkee, Roorkee 247 667 U.P.

ACKNOWLEDGEMENT

I would like to express my deep sense of gratitude to my guide Dr. P.K. Ghosh, Scientist (Professor), Department of Mechanical and Industrial Engineering, University of Roorkee, Roorkee for his valuable guidance and generous help at all stages of this study. His meticulous care in going through the manuscript and valuable suggestions are greatly acknowledged. My sincere thanks are due to Dr. S.R. Gupta, Professor, Department of Mechanical and Industrial Engineering, University of Roorkee, Roorkee for his constant encouragement and for extending all facilities.

Thanks are due to Dr. J.S. Saini, Professor and Head of the Department of Mechanical and Industrial Engineering, University of Roorkee, Roorkee for providing me with the necessary facilities for conducting this work.

My sincere thanks are due to Mr. A.K. Mithal, AGM(QM), CFFP, BHEL, Hardwar for his constant encouragement to complete this work.

Thanks are due to Shri D.K. Kapil and Shri S.M. Mishra for helping me all the way during the course of this work. I am also thankful to Mr. Vivek Gupta and Mr. Tushar Dave, Engineers, CFFP, BHEL, Hardwar for their help in completing this work. Finally, I owe to all my friends and well wishers who have made this endeavour worthwhile.

Date : October 3rd, 1997


(V.K. AGARWAL)

Roorkee

ABSTRACT

Repair welding of C-Mn steel shaft forgings was carried out under simulated conditions of repairing, using different welding parameters and post weld heat treatment. The welding parameters were varied as preheat temperature, dia of electrodes and duration of post weld heat treatment at a given temperature of 510 °C. The repairing works were carried out as per ASME Section IX. Microstructure and mechanical properties of weld joints such as its hardness, tensile strength and fatigue life were studied. It was observed that the use of low preheating and smaller dia of electrodes reduces grain coarsening of heat affected zone during post weld heat treatment due to promotion of martensite transformation in it. The increase in preheating temperature and size of electrode has been found to enhance the coarsening of grain size and pearlite colonies in the weld deposit during post weld heat treatment of the weld. During the use of higher size of electrodes weld joints were mostly found to fracture from base metal under tensile test of weld joints. During fatigue testing, the weld joints are always found to fracture from base material.

Thus the fatigue properties of the weld could not be identified. However it is marked that under the present conditions of welding used in this investigation, fatigue properties of weld are superior to those of base material.

LIST OF TABLES

| TABLE NO. | TITLE | PAGE NO. |
|-----------|--|----------|
| 2.1 | Chemical composition of C-Mn steel forgings | 5 |
| 2.2 | Mechanical properties of C-Mn steel forgings | 6 |
| 2.3 | Parameters for air arc gouging | 11 |
| 2.4 | Cooling time Carbon equivalent formula for C-Mn steel forgings | 14 |
| 3.1 | Chemical composition of base material | 42 |
| 3.2 | Mechanical properties of base material | 43 |
| 3.3 | Chemical composition of filler metal | 44 |
| 3.4 | Welding parameters and specimen designation | 47 |
| 4.1 | Mechanical properties of base material | 57 |
| 4.2 | Results of measurements of width of HAZ | 62 |
| 4.3 | Results of hardness measurements of HAZ | 70 |
| 4.4 | Results of fatigue tests carried out on welded specimens | 79 |

at a maximum stress of 370 N/mm² and R=0.1

LIST OF FIGURES

| FIGURE NO. | TITLE | PAGE NO. |
|------------|--|----------|
| 2.1(a) | Cooling time 800-500 °C on weld metal microstructure at a post weld heat treatment of 510 °C for 10 hrs using O3.15 mm electrodes C for 250 DPH maximum hardness related to C equivalent | 15 |
| 2.1(b) | Cooling time 800-500 °C for 300 DPH maximum hardness related to C equivalent | 15 |
| 2.1(c) | Cooling time 800-500 °C for 350 DPH maximum hardness related to C equivalent | 15 |
| 2.2 | Nomogram for calculating preheat temperature | 16 |
| 2.3 | Schematic microstructure of C and low alloy steel weldment | 19 |
| 2.4 | Buttering technique | 20 |
| 2.5 | Effect of temperature on stress relief | 23 |
| 2.6 | Effect of temperature & time on stress relief | 24 |
| 2.7 | Thermal cycles experienced by indicated locations in the heat affected zone of an arc weld made with 100 kJ/inch for ½ inch steel plate at room temperature. | 27 |
| 2.8 | Effect of initial plate temperature on thermal cycle | 28 |
| 2.9 | Effect of initial plate temperature and energy input on thermal cycles in HAZ of arc weld | 31 |
| 2.10 | Transverse shrinkage | 32 |
| 2.11 | Angular distortion | 32 |
| 2.12 | Longitudinal shrinkage | 32 |
| 2.13 | Angular distortion in fillet welds | 32 |
| 2.14 | Angular distortion in fillet welds | 32 |

| | | |
|------|--|----|
| 2.15 | Distribution of longitudinal stresses | 37 |
| 3.1 | Schematic diagram of collection of test plates and their edge preparation | 41 |
| 3.2 | Fixture for welding of plates | 48 |
| 3.3 | Sectioning plan for preparation of samples | 49 |
| 3.4 | Diagram showing the machining thickness from both sides for specimen fabrication | 50 |
| 3.5 | Diagram showing the dimension of tensile specimen | 51 |
| 3.6 | Diagram showing the dimension of fatigue specimen | 51 |
| 4.1 | Microstructures of base metal at 200x | 56 |
| 4.2 | Micrographs showing the effect of preheating (a,b,c) on weld metal microstructure at a post weld heat treatment of 510 °C for 5 hrs using ϕ 3.15mm electrodes | 58 |
| 4.3 | Micrographs showing the effect of preheating (a,b,c) on weld metal microstructure at a post weld heat treatment of 510 °C for 10 hrs using ϕ 3.15 mm electrodes | 59 |
| 4.4 | Micrographs showing the effect of preheating (a,b,c) on weld metal microstructure at a post weld heat treatment of 510 °C for 5 hrs using ϕ 5.00 mm electrodes | 60 |
| 4.5 | Micrographs showing the effect of preheating (a,b,c) on weld metal microstructure at a post weld heat treatment of 510 °C for 10 hrs using ϕ 5.00 mm electrodes | 61 |
| 4.6 | Effect of preheat temperature on the width of HAZ using ϕ 5.00 mm electrodes | 63 |
| 4.7 | Effect of preheat temperature on the width of HAZ using ϕ 3.15 mm electrodes | 63 |

| | | |
|------|--|----|
| 4.8 | Micrographs showing the effect of preheat (a,b,c) temperature on HAZ microstructure at a post weld heat treatment of 510 °C for 5 hrs using ϕ 3.15 mm electrodes | 66 |
| 4.9 | Micrographs showing the effect of preheat (a,b,c) temperature on HAZ microstructure at a post weld heat treatment of 510 °C for 10 hrs using ϕ 3.15 mm electrodes | 67 |
| 4.10 | Micrographs showing the effect of preheat (a,b,c) temperature on HAZ microstructure at a post weld heat treatment of 510 °C for 5 hrs using ϕ 5.00 mm electrodes | 68 |
| 4.11 | Micrographs showing the effect of preheat (a,b,c) temperature on HAZ microstructure at a post weld heat treatment of 510 °C for 10 hrs using ϕ 5.00 mm electrodes | 69 |
| 4.12 | Effect of preheat temperature on HAZ hardness using ϕ 3.15 mm electrodes | 71 |
| 4.13 | Effect of preheat temperature on HAZ hardness of HAZ using ϕ 5.00 mm electrodes | 71 |
| 4.14 | Typical tensile load displacement behaviour of weld joints | 72 |
| 4.15 | Effect of preheat temperature and duration of PWHT on UTS of weld joints using ϕ 3.15 electrodes | 75 |
| 4.16 | Effect of preheat temperature and duration of PWHT on UTS of weld joints using ϕ 5.00 electrodes | 76 |
| 4.17 | Effect of preheat temperature and duration of PWHT on fatigue life of weld joints using ϕ 3.15 electrodes | 77 |
| 4.18 | Effect of preheat temperature and duration of PWHT on fatigue life of weld joints using ϕ 5.00 electrodes | 78 |

CONTENTS

PAGE NO.

CERTIFICATE

ACKNOWLEDGEMENT

ABSTRACT

LIST OF TABLES

LIST OF FIGURES

CHAPTER

| | | |
|----|--|----|
| 1. | INTRODUCTION | 1 |
| 2. | LITERATURE REVIEW | 3 |
| | 2.1 Chemical composition and Mechanical Properties of C-Mn steel forgings. | 3 |
| | 2.2 Quality Assurance of C-Mn steel forgings | 3 |
| | 2.3 Identification of defects | 4 |
| | 2.3.1 Non-Destructive Testing of steel forgings | 4 |
| | 2.3.2 Type of defects found in C-Mn steel forgings | 7 |
| | 2.4 Defect removal | 9 |
| | 2.4.1 Excavation of defects | 9 |
| | 2.4.2 Post excavation NDT | 10 |
| | 2.5 Repair welding | 10 |
| | 2.5.1 Repair welding consumables | 10 |

| | | |
|---------|----------------------------------|----|
| 2.5.1 | Repair welding consumables | 10 |
| 2.5.2 | Repair welding processes | 12 |
| 2.5.3 | Repair welding procedures | 12 |
| 2.5.3.1 | Preheat | 12 |
| 2.5.3.2 | Welding sequence | 18 |
| 2.5.3.3 | Post weld heat treatment | 21 |
| 2.5.4 | Post repairing NDT | 21 |
| 2.6 | Weld thermal cycles | 22 |
| 2.7 | Distortion and residual stresses | 29 |
| 2.8 | Cost of repairing | 35 |
| 3. | EXPERIMENTATION | 39 |
| 3.1 | Base material | 39 |
| 3.2 | Filler metal | 39 |
| 3.3 | Welding equipment | 39 |
| 3.4 | Welding of plates | 40 |
| 3.4.1 | Edge preparation | 40 |
| 3.4.2 | NDT of plates | 40 |
| 3.4.3 | Welding | 45 |
| 3.4.4 | NDT of welded plates | 45 |
| 3.4.5 | Post weld heat treatment | 46 |
| 3.5 | Mechanical testing | 46 |
| 3.5.1 | Specimen collection | 46 |

| | | |
|---------|-----------------------------------|----|
| 3.5.2 | Tensile test | 46 |
| 3.5.2.1 | Tensile test of base material | 52 |
| 3.5.2.2 | Tensile test of weld joint | 52 |
| 3.5.3 | Fatigue test of weld joints | 52 |
| 3.6 | Metallography examination | 53 |
| 3.6.1 | Optical metallography | 53 |
| 3.7 | Hardness measurement | 53 |
| 4. | RESULTS AND DISCUSSION | 54 |
| 4.1 | Base metal properties | 54 |
| 4.1.1 | Microstructure | 54 |
| 4.1.2 | Mechanical properties | 54 |
| 4.2 | Microstructure of weld metal | 55 |
| 4.3 | Microstructure of HAZ | 56 |
| 4.4 | Hardness of HAZ | 64 |
| 4.5 | Tensile properties of weld joints | 65 |
| 4.6 | Fatigue properties of weld joints | 73 |
| 5. | CONCLUSIONS | 80 |
| | SCOPE FOR FUTURE WORK | 81 |
| | REFERENCES. | 82 |

CHAPTER-1

1.0 INTRODUCTION

During manufacture of steel forgings, several defects are encountered, such as seams, laps, inclusions, segregations, cracks, bursts, folds, cold shuts. Repair of forging defects by welding is generally not recommended due to fatigue considerations. However depending on the severity of the defects, their location and orientation as detected by Non Destructive Testing (NDT) methods, repair of certain defects by welding may be undertaken. Repairing by fusion welding often poses certain problems due to weld thermal cycles. But by proper selection of welding process/procedure/parameters, welding consumables, preheat temperatures, welding technique, post heat maintenance and post weld heat treatment, repair welding of forgings may be carried out successfully. Steps involved in repair welding of forgings. The steps involved in repair welding of forgings can be broadly classified as follows.

- a) First step involved is the detection of forging defects by NDT methods viz ultrasonic test, dye penetrant testing and magnetic particle examination.
- b) Removal of defect by air arc gouging/grinding/pneumatic chipping.
- c) Non-destructive examination of excavations to ensure freedom from defects.
- d) Repair welding.

- e) NDT of weldments and adjoining Heat Affected Zone (HAZ).
- f) Post-weld heat treatment.
- g) NDT of weld-repair zones and adjoining areas.
- h) Machining, if required.

In the present investigation, an attempt is made to evaluate the influence of various key aspects of repair welding like preheating and heat input on microstructure as well as static and dynamic properties of weld and HAZ of C-Mn steel forgings. This investigation is targetted towards finding out a suitable repair welding procedure which may be effectively used in case of repair welding of steel forgings for critical applications enjoying dynamic loading conditions in servion.

CHAPTER-2

LITERATURE REVIEW

2.1 CHEMICAL COMPOSITION AND MECHANICAL PROPERTIES OF C-Mn STEEL FORGINGS.

C content of C-Mn steel forgings lies in the range of .2-5%, S and P is maintained in the range of 0.04 max. and 0.04% respectively, Si is maintained in the range of .15-.35% and Mn in the range of 0.5-1.75%. The role of C and Mn is primarily to provide strengthening to the matrix. Mn lowers the AR3 and AR1 temperatures and increases hardenability. Mn upto .8% dissolves in iron, any manganese in excess of this quantity forms Mn_3C which occurs with Fe_3C . These forgings are generally normalised and tempered. Microstructure of these forgings consist of ferrite and pearlite. These forgings are especially used for Hydro-Tur-bine components.

In C-steel forgings, with increase in C content yield strength (YS), Ultimate tensile strength (UTS) and hardness increases, % elongation and % reduction in area decreases. In .2% C steel forgings, YS is achieved in the range of 230 N/mm^2 min., UTS 430 N/mm^2 , and %elongation 24% min. In .3% C steel forgings, YS is achieved in the range 270 N/mm^2 min, UTS 490 N/mm^2 min. and % Elongation 21%. With addition of 1.5% Mn in C steel, YS, UTS and hardness increases. In .2% C, 1.5% Mn steel YS and UTS is achieved in the range of 300 and 500 N/mm^2 min. respectively. Chemical composition and mechanical properties of C-Mn steel forgings are as per table 2.1 and 2.2 respectively.

2.2 QUALITY ASSURANCE OF STEEL FORGINGS

Limit for acceptable flaws in steel forgings is stringent as compared to other engineering steel components such as steel castings. Following are flaws acceptance norms for C-Mn steel forgings.

1. Cracks and flakes not allowed.
2. All isolated indications with equivalent flaw size > 4 mm not acceptable.
3. All flaw indications with back echo loss > 4 db unacceptable.
4. Flaws with equivalent flaw size > 3 mm with length > 20 mm unacceptable.

2.3 IDENTIFICATION OF DEFECTS

2.3.1 Non-Destructive Testing of steel forgings

All repairs must have a sound foundation. Therefore it is essential that the testing must be carried out carefully to find out even the smallest crack or defect present in a forged component. Mainly liquid penetrant, magnetic particle and ultra-sonics are used as examination methods.[2,3] For magnetic particle testing of machined forgings, Yoke methods are used, since yoke method does not cause localized heating. For detection of surface defects AC yokes with lifting power of 5 kgs are used and for detection of sub-surface and surface defects, DC yokes with lifting power of 18 kgs are used. For detection of defects open to surface, liquid penetrant method is used. In this method the area to be tested is cleaned and then sprayed with a low viscosity dye penetrant which is red in colour. After approximately 30 minutes, the excess dye is washed off and chalk developer is applied. Developer acts as a blotting paper, absorbs any dye

TABLE 2.1

CHEMICAL COMPOSITION OF C- Mn STEEL FORGINGS

| SPECIFICATION | C | S | P | Si | Mn | Ni | Cr | Mo | V | Cu | Sn |
|---------------|------|-------|-------|------|------|------|------|------|------|------|------|
| AA10124/CL2 | 0.15 | 0.04 | 0.04 | 0.15 | 0.60 | 0.25 | 0.25 | 0.15 | 0.05 | 0.35 | 0.05 |
| | 0.25 | max. | max. | max. | 0.90 | 0.35 | max. | max. | max. | max. | max. |
| AA10127/CL3 | 0.25 | 0.04 | 0.04 | 0.15 | 0.60 | 0.30 | 0.30 | 0.15 | 0.05 | 0.35 | 0.05 |
| | 0.35 | max. | max. | 0.35 | 0.90 | max. | max. | max. | max. | max. | max. |
| AA10128/CL4 | 0.40 | 0.04 | 0.04 | 0.15 | 0.60 | 0.25 | 0.25 | 0.15 | 0.05 | 0.35 | 0.05 |
| | 0.50 | max. | max. | max. | 0.90 | 0.35 | max. | max. | max. | max. | max. |
| AA19341 | 0.16 | 0.035 | 0.035 | 0.10 | 1.30 | 0.30 | 0.30 | 0.15 | 0.05 | 0.25 | 0.05 |
| | 0.24 | max. | max. | 0.35 | 1.70 | max. | max. | max. | max. | max. | max. |
| AA19342 | 0.24 | 0.035 | 0.035 | 0.10 | 1.30 | 0.30 | 0.30 | 0.15 | 0.05 | 0.25 | 0.05 |
| | 0.32 | max. | max. | 0.35 | 1.70 | max. | max. | max. | max. | max. | max. |

NOTE : Chemical composition in %

penetrated into the defects open to the surface revealing an image of the flaws on the surface. [2]For detection of internal defects ultrasonic test is used. Pulse echo method is used in ultrasonic testing. Surface finish for testing should be in between 6.25 microns to 12.5 microns. These test is carried out after quality heat treatment. Ultra-sonic probes of 1-5 MHz frequency are used. For defect sizing, distance gain size diagrams (DGS) appropriate to the type of probes are used. Oil and grease are used as couplants. Coupling agents should not cause any corrosive damages. Speed of scanning should not exceed 100 mm/sec. There should be an overlap of minimum 15% in subsequent runs. Echo indications are characterized by echo amplitude, extended length, possibly their dynamic behaviour and frequency dependence. Back echo loss if any must also be estimated.

Radiography of forging is not recommended because of higher thickness of forgings and geometry of defects observed in forging are comparatively very thin due to forging operation and are difficult to be detected by Radiography methods.

2.3.2 Type of defects found in steel forgings

Defects found in steel forgings can be broadly classified into two groups.

A. Defects arising from the cast ingot.

B. Processing defects.

A. Defects arising from cast ingots.

Following defects are observed in steel forgings in this group.

i) Pulls :

Clearly visible transverse cracks due to cracks present in ingots having opened up during cogging.

ii) Splits :

Longitudinal cracks, sometimes difficult to see with naked eye, these may be along the corner or at the center of the face.

iii) Shells :

Relatively thin flakes or tongues of metal, imperfectly attached to the surface, resulting from the ingot defects like double skin, splash, flash or fin.

iv) Broken corners:

Breaking of corners due to exposure and oxidation of sub-cutaneous blowholes, mostly apparent at corners.

v) Sand :

Massive non-metallic inclusions visible to naked eyes during machining, results from segregation of oxidizing products particularly alumina. Also known as dust or nonmetallic inclusion.

vi) Seams :

Numerous shallow grooves or striations formed during upsetting of oxidized surface.

B. Processing defects :

Following defects are observed in this group.

TABLE 2.1**CHEMICAL COMPOSITION OF C- Mn STEEL FORGINGS**

| SPECIFICATION | C | S | P | Si | Mn | Ni | Cr | Mo | V | Cu | Sn |
|---------------|------|-------|-------|------|------|------|------|------|------|------|------|
| AA10124/CL2 | 0.15 | 0.04 | 0.04 | 0.15 | 0.60 | 0.25 | 0.25 | 0.15 | 0.05 | 0.35 | 0.05 |
| | 0.25 | max. | max. | max. | 0.90 | 0.35 | max. | max. | max. | max. | max. |
| AA10127/CL3 | 0.25 | 0.04 | 0.04 | 0.15 | 0.60 | 0.30 | 0.30 | 0.15 | 0.05 | 0.35 | 0.05 |
| | 0.35 | max. | max. | 0.35 | 0.90 | max. | max. | max. | max. | max. | max. |
| AA10128/CL4 | 0.40 | 0.04 | 0.04 | 0.15 | 0.60 | 0.25 | 0.25 | 0.15 | 0.05 | 0.35 | 0.05 |
| | 0.50 | max. | max. | max. | 0.90 | 0.35 | max. | max. | max. | max. | max. |
| AA19341 | 0.16 | 0.035 | 0.035 | 0.10 | 1.30 | 0.30 | 0.30 | 0.15 | 0.05 | 0.25 | 0.05 |
| | 0.24 | max. | max. | 0.35 | 1.70 | max. | max. | max. | max. | max. | max. |
| AA19342 | 0.24 | 0.035 | 0.035 | 0.10 | 1.30 | 0.30 | 0.30 | 0.15 | 0.05 | 0.25 | 0.05 |
| | 0.32 | max. | max. | 0.35 | 1.70 | max. | max. | max. | max. | max. | max. |

NOTE : Chemical composition in %

TABLE 2.2

MECHANICAL PROPERTIES OF C-Mn STEEL FORGINGS

| SPECIFICATION | YS (min) (N/mm2) | UTS (min) (N/mm2) | %El (min) (l=5d) | %RA | BHN | IMPACT STRENGTH (min)(J) (2 mm U) |
|----------------------|------------------------------------|-------------------------------------|--|------------|----------------|---|
| AA10124/CL2 | 230 | 430 | 24.0 | - | - | - |
| AA10127/CL3 | 270 | 490 | 21.0 | - | - | - |
| AA10128/CL4 | 320 | 620 | 15.0 | - | - | - |
| AA19341 | 295 | 510 | 17.0 | - | 143-197 | 31.4 |
| AA19342 | 335 | 560 | 16.0 | - | 156-212 | 39.2 |

penetrated into the defects open to the surface revealing an image of the flaws on the surface. [2]For detection of internal defects ultrasonic test is used. Pulse echo method is used in ultrasonic testing. Surface finish for testing should be in between 6.25 microns to 12.5 microns. These test is carried out after quality heat treatment. Ultra-sonic probes of 1-5 MHz frequency are used. For defect sizing, distance gain size diagrams (DGS) appropriate to the type of probes are used. Oil and grease are used as couplants. Coupling agents should not cause any corrosive damages. Speed of scanning should not exceed 100 mm/sec. There should be an overlap of minimum 15% in subsequent runs. Echo indications are characterized by echo amplitude, extended length, possibly their dynamic behaviour and frequency dependence. Back echo loss if any must also be estimated.

Radiography of forging is not recommended because of higher thickness of forgings and geometry of defects observed in forging are comparatively very thin due to forging operation and are difficult to be detected by Radiography methods.

2.3.2 Type of defects found in steel forgings

Defects found in steel forgings can be broadly classified into two groups.

A. Defects arising from the cast ingot.

B. Processing defects.

A. Defects arising from cast ingots.

Following defects are observed in steel forgings in this group.

i) Pulls :

Clearly visible transverse cracks due to cracks present in ingots having opened up during cogging.

ii) Splits :

Longitudinal cracks, sometimes difficult to see with naked eye, these may be along the corner or at the center of the face.

iii) Shells :

Relatively thin flakes or tongues of metal, imperfectly attached to the surface, resulting from the ingot defects like double skin, splash, flash or fin,

iv) Broken corners:

Breaking of corners due to exposure and oxidation of sub-cutaneous blowholes, mostly apparent at corners.

v) Sand :

Massive non-metallic inclusions visible to naked eyes during machining, results from segregation of oxidizing products particularly alumina. Also known as dust or nonmetallic inclusion.

vi) Seams :

Numerous shallow grooves or striations formed during upsetting of oxidized surface.

B. Processing defects :

Following defects are observed in this group.

i) Laps :

Oxidized folds in the skin.

ii) Overfilled :

When two large reduction is attempted or material is not hot enough, a rib or fin is formed on both sides.

iii) Underfilled :

When less material is present.

iv) Burnt :

Produced in reheating furnaces, when reheating to too high a temperature. Present in the form of irregular disintegration of affected part.

v) Hot shortness :

Breaking of steels during forging due to steels high in sulfur with insufficient Mn, steels high in Phosphorus and steels contaminated with large quantities of Sn and Cu.

2.4 DEFECT REMOVAL

2.4.1 Excavation of defects

For removal of cracks grinding is recommended [2]. For removal of defects, other methods used are pneumatic chipping and air arc gouging. Removal of defects near to the surface is done by grinding or pneumatic chipping. The deep seated defects are removed by air arc gouging. Air arc gouging electrodes are made of graphite and carbon. These electrodes are clad with copper of 0.5 mm thickness. Rods are available in following sizes as per table 2.3. Before air arc gouging, C-Mn steel forgings are preheated locally to 150°C. After removal of defects by air arc gouging

about 2 mm deep metal is further removed by grinding to remove the carbon pickup zones of the excavations.

2.4.2 Post excavation NDT

After defect removal and preparation of excavations by grinding these are checked by LPI/MP to ensure defect free surfaces.

2.5 REPAIR WELDING

2.5.1 Repair welding Consumables

Filler material is added to fusion welded joints and weld deposit consists of a mixture of parent metal and filler metal. Mixing of parent metal into the filler metal results in dilution (D) of weld deposit. The dilution D is estimated as

$$D = \frac{\text{Wt. of parent metal melted}}{\text{Total wt. of fused metal}} \times 100 \%$$

Degree of dilution depends upon the groove geometry, the edge preparation and the process used. It becomes maximum for single run weld deposits on thin section with square edge preparation and minimum in case of multipass weld deposit with a normal edge preparation [4]. Dilution effects are significant in case of repair welding of higher carbon content forgings especially for root runs, which results into higher carbon weldment, prone to cracking. For this purpose it is recommended to use basic coated electrodes with shielded metal arc welding process for root run for heavy weldments of high carbon content steel forgings [5].

TABLE 2.3
PARAMETERS USED FOR AIR ARC GOUGING

| ELECTRODE SIZE | TYPICAL CURRENT | TYPICAL AIR PRESSURE | AMOUNT OF METAL USED/RUN |
|-------------------|--------------------|-------------------------|-----------------------------|
| (mm) | (Amp) | (Kg/cm ²) | (mm) |
| ∅ 6.0 | 350 | 4 | 2 |
| ∅ 9.0 | 450 | 6 | 4 |
| ∅ 12.0 | 600 | 8 | 5 |
| 5x20 | 450 | 6 | 3 |

Criteria for selection of filler metals is based on matching properties of weld metals to parent metals. In this regard most widely used code in industry is ASME Sec II.SFA 5.5- For C-Mn steel forgings. For repair welding of C-Mn steel forgings the recommended consumable using SMAW process is Supratherme (special) E7018-1Ø3.15, Ø4.00 and Ø5.00 mm

2.5.2 Repair Welding processes

Choice of welding processes generally depends upon the size and number of components, amount of repair, and availability of positioning equipments. SMAW requires the least amount of equipments and provides maximum flexibility for welding in remote locations and in all positions. Semi-automatic welding processes which use wire feeders and self shielded flux cored wires give high deposition rates. For repairing of massive forgings, flux cored arc welding and SMAW processes are often used [7]. The increased penetration of submerged arc welding process compared with the SMAW process is advantageous for welding of low carbon steel forgings, because the weldment soundness is enhanced. However it is disadvantageous when welding the higher carbon content steel forgings, because of increased weld metal carbon content resulting therefrom [5].

2.5.3 Repair Welding procedures

Welding procedures consist of preheat temperature , interpass temperature , preheat maintenance , welding technique and post weld heat treatment.

2.5.3.1 Preheat

Majority of the steel forgings are of sufficient thickness. The thicker sections have greater heat absorbing capacities and therefore it has greater

quenching power. Hence in order to reduce the cooling rates and the hardness of the parent metal/weld metal boundary preheating is required. The cooling rate from austenitization necessary to produce a martensitic structure is called the critical cooling rate. First step in deciding preheat temperature is to determine whether the critical cooling rate, under welding conditions will be exceeded and if so whether preheating will enable the actual cooling rate to be held below the critical cooling rate. For determination of critical cooling rate, the cooling time C equivalent is calculated. For C-Mn steel forgings, cooling time C equivalent is calculated using the formula in table 2.4. Having calculated the equivalent carbon of the particular steel under consideration, the critical cooling time for this equivalent carbon is calculated from figure 2.1. By using the nomogram given in figure 2.2 preheat temperature necessary to avoid exceeding critical cooling rate is determined. Avoiding root run delayed cracking require local preheating whether or not general preheat for control of cooling rate is necessary when welding forgings of C-Mn steel. For welding of .2% C - 1.5% Mn steels with Ø3.15 mm electrodes with heat input of approximate 10 KJ/cm preheat of the order of 250°C and with Ø5.00 mm electrodes with heat input of approximately 16 KJ/cm, preheat of approximately 150°C is required [5]. A higher level of preheat helps to reduce internal stresses set up during welding, specially where the size of weld requires specific procedure to control distortion and reduce stress level [10].

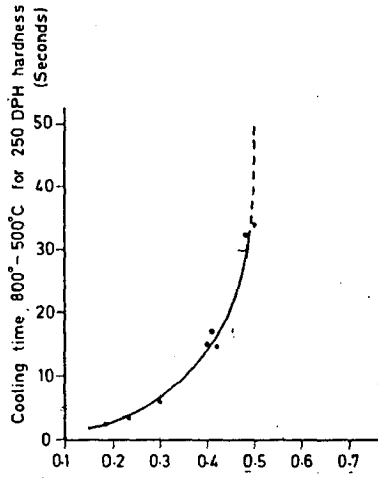
On large forgings where preheating inside the furnace is not possible it is carried locally with gas burners or electrical resistance heating pads. Preheat can be measured either by thermocouple or temperature indicating crayons at the surface farthest away from the heat source to ensure that the heat has penetrated through the full thickness of the section [10]. Heat affected zone is the region of the parent metal near to the fusion line, i.e,

TABLE 2.4

COOLING TIME C EQUIVALENT FORMULA FOR C-Mn STEEL FORGINGS

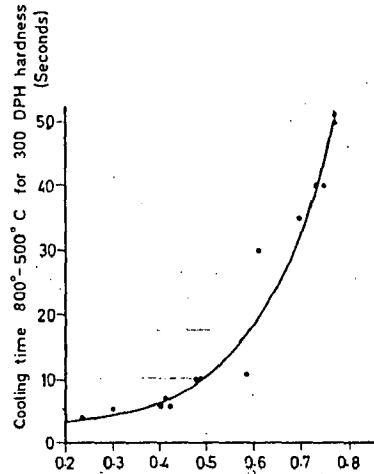
| CARBON RANGE | FOR HAZ MAXIMUM HARDNESS 250 DPH | FOR HAZ MAXIMUM HARDNESS 300 DPH OR 350 DPH |
|--------------|---|--|
| UPTO 0.2 | Si Mn Ni Cr Mo C+--+--+--+--+-- 4 15 19 6.5 3 | Si Mn Ni Cr Mo C+--+--+--+--+-- 4 5 11 7 3 |
| 0.21-0.3 | Mn Ni Cr Mo C+--+--+--+--+-- 4 7 19 3 | Si Mn Ni Cr Mo C+--+--+--+--+-- 4 3.5 11 7 3 |
| 0.31-0.4 | Si Mn Ni Cr C+--+--+--+--+-- 4 4 7 15 | Si Mn Ni Cr Mo C+--+--+--+--+-- 4 3.5 9 3 2 |

FIG.2.1(a) Cooling time 800-500°C
For 250 DPH Maximum hardness
related to carbon equivalent

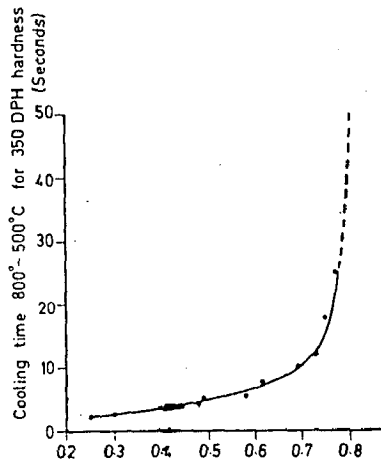


Carbon Equivalent :-

FIG. 2.1(b) Cooling time 800-500°C
For 350 DPH Maximum hardness
related to carbon equivalent



Carbon Equivalent :-



Carbon Equivalent :-

Fig. 2.1(c) Cooling time 800-500°C
For 350 DPH Maximum hardness
related to carbon equivalent

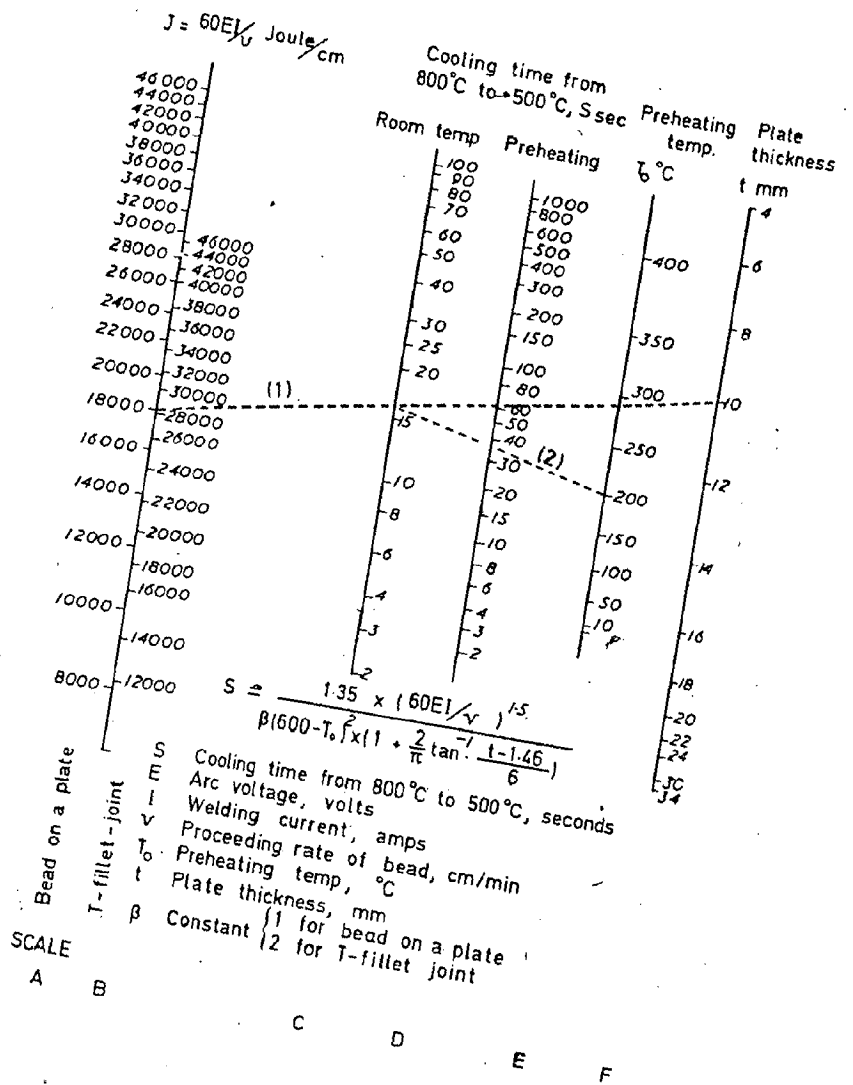


Fig. 2.2
**NOMOGRAM FOR CALCULATING PREHEAT
 TEMP.**

heated to a temperature equal to AC1 or higher. Near the fusion line, temperature is close to the melting point. HAZ can be further subdivided into three zones as shown in fig. 2.3.

1. Coarse grain zone

This zone is also known as high temperature zone. Final grain size in this region will depend upon the peak temperature to which it is exposed and the residence time. For isothermal heating, the final mean grain size d_t is given by

$$d_t^n = Kt + d_0^n$$

where t is the time and d_0 is the initial grain size. K and n are constants.

Final grain size will increase with increasing peak temperature and residence time. The maximum peak temperature is melting point. The only significant variable therefore is residence time. Residence time is proportional to the heat input rate. Transformation of coarse grain austenite is delayed to lower temperatures as compared to fine grain austenite. In C-Mn steel coarse grain zone of HAZ produces a harder structure than would be obtained from conventional heat treatment quenching practice using the same cooling rate where the grain size is not coarse.

2. Fine grain zone

In this zone, austenite grains are not coarsened. This zone consist of bainite and carbide precipitates.

3. Mixed structure

In this zone, the temperature during heating lies in between AC1 and AC3 and austenite is formed partially. On cooling, there forms a mixed structure in this zone. In no circumstances the interpass temperature should be allowed to fall below preheat temperature. It should not be allowed to go so high as to impair the strength of deposited weld metal.

2.5.3.2 Welding Sequence :

In repairs requiring large volume of weld metal, the effect of the induced stresses may be offset by using a block technique in which the weld is built up by intermittent blocks which are subsequently joined together by others after the first group is completed. Benefit of this technique is that it reduces longitudinal stresses. It does not have much effect on transverse stresses [10]. To reduce the effect of shrinkage stress, a buttering technique can be employed. This method allows weld runs to be deposited progressively on the prepared faces of excavations, prior to bridging the final gap between them. This reduces as far as possible the induced strain in the parent metal caused by the contraction of the weld metal. Refer fig 2.4. It is recommended that the weld should be made using stringer techniques. This technique, owing to the small volume of metal deposition, will not induce high shrinkage stresses as it occurs in case of weave technique. To take into account the heat cracking, and distortion problem, molten pool is kept as small as possible with $\phi 3.15$ mm electrode, moderate currents and stringer beads. Every stringer bead in hot state is compressed out by peening with compressed air tool to prevent shrinkage in volume.

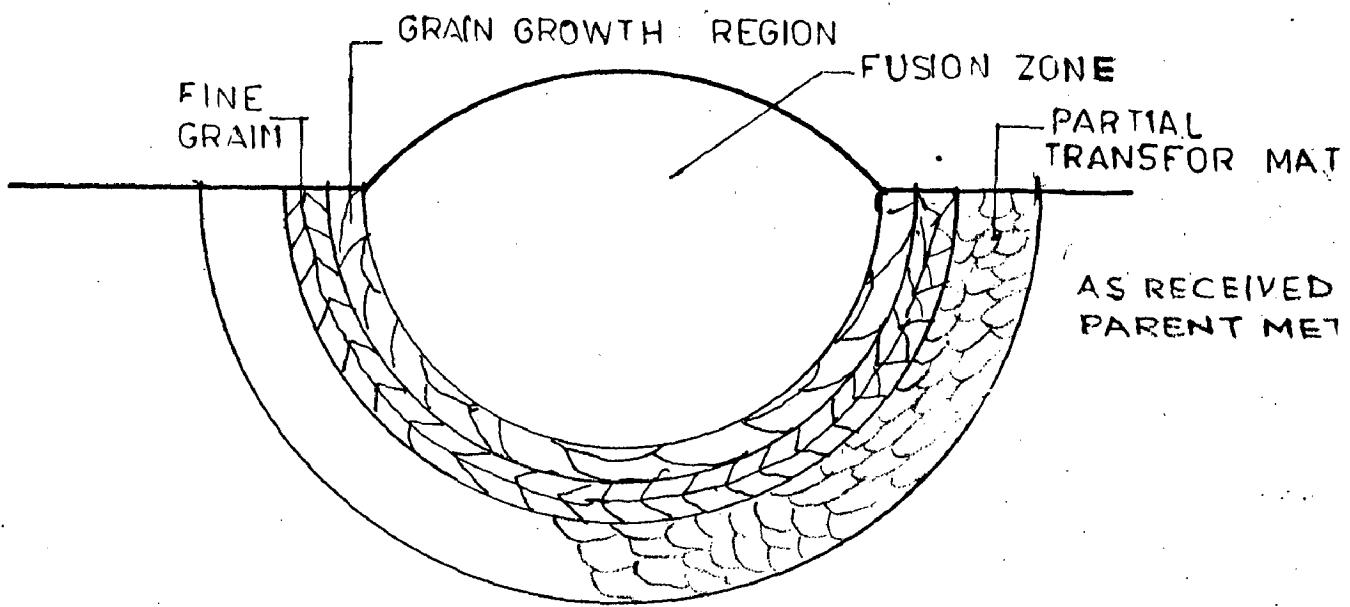


FIG 2.3 SCHEMATIC MICRO STRUCTURE OF CARBO AND LOW ALLOY STEEL WELDMENT.

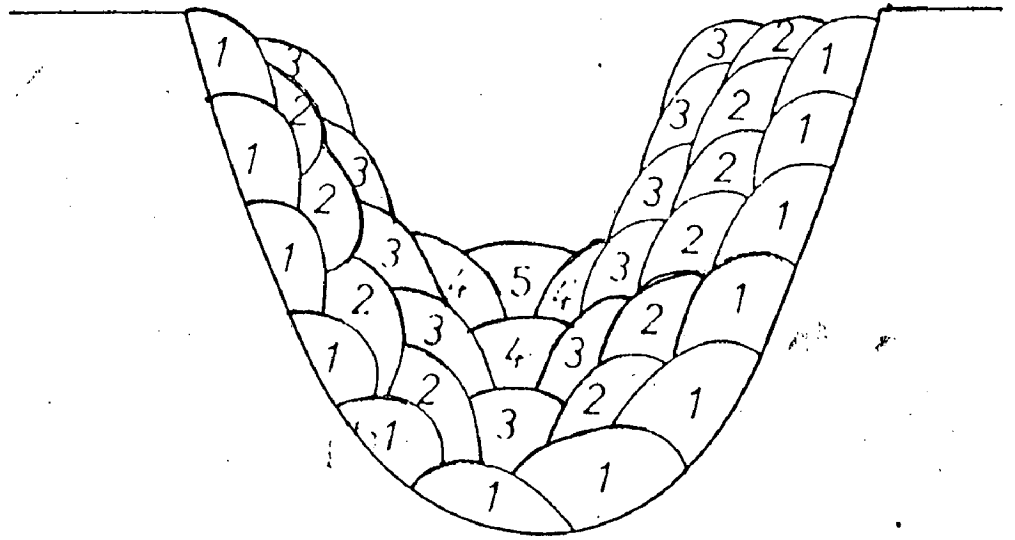


FIG 2.4 : BUTTERING TECHNIQUE

2.5.3.3 Post Weld Heat Treatment

It consists of heating at a controlled rate to a suitable temperature that is below the critical range of the base metal, followed by controlled cooling. Advantages of stress relieved repair are that the stress relief reduces residual stresses, increases the ductility of the heat affected zone and reduces embrittlement of the material. It also lowers the fracture appearance transition temperature [6]. The reduction of the "metallurgical notch" effect resulting from abrupt changes in hardness or other microstructural discontinuities around weld can be readily accomplished by correct post weld heat treatment. Resistance to the propagation of cracks specially in the heat affected zone adjacent to the weld is often directly related to correct welding procedure including post weld heat treatment [11]. The residual stresses remaining in the material after thermal stress relieve will depend upon the cooling rate. Uneven cooling from stress relief to ambient temperature may undo much of the value of stress relieving and may result in additional stresses in the weldment. Effect of varying stress relieving temperature and time on percentage relief of residual stresses are as shown in figures 2.5 and 2.6.

2.5.4 Post repairing NDT

After weld repair, the repaired zones and the adjoining areas are checked by liquid penetrant method / magnetic particle method and ultrasonic to ensure sound weldments.

2.6 WELD THERMAL CYCLES

For a single pass full penetration butt weld in a sheet or plate the distribution of peak temp. in base metal adjacent to the weld is given by

$$\frac{1}{T_p - T_o} = \frac{4.13 \rho c t Y}{h(\text{net})} + \frac{1}{T_m - T_o}$$

where T_p = peak temp. in °C at a distance Y from the fusion line

T_o = initial uniform temp.

T_m = melting point of base metal

$h(\text{net})$ = net energy input = $f_1 EI/V$

E = arc voltage in volts, I = welding current in amperes, V = welding travel speed, f_1 = heat transfer efficiency

ρ = density of material

c = specific heat of material

t = thickness

This equation can be used for estimating the

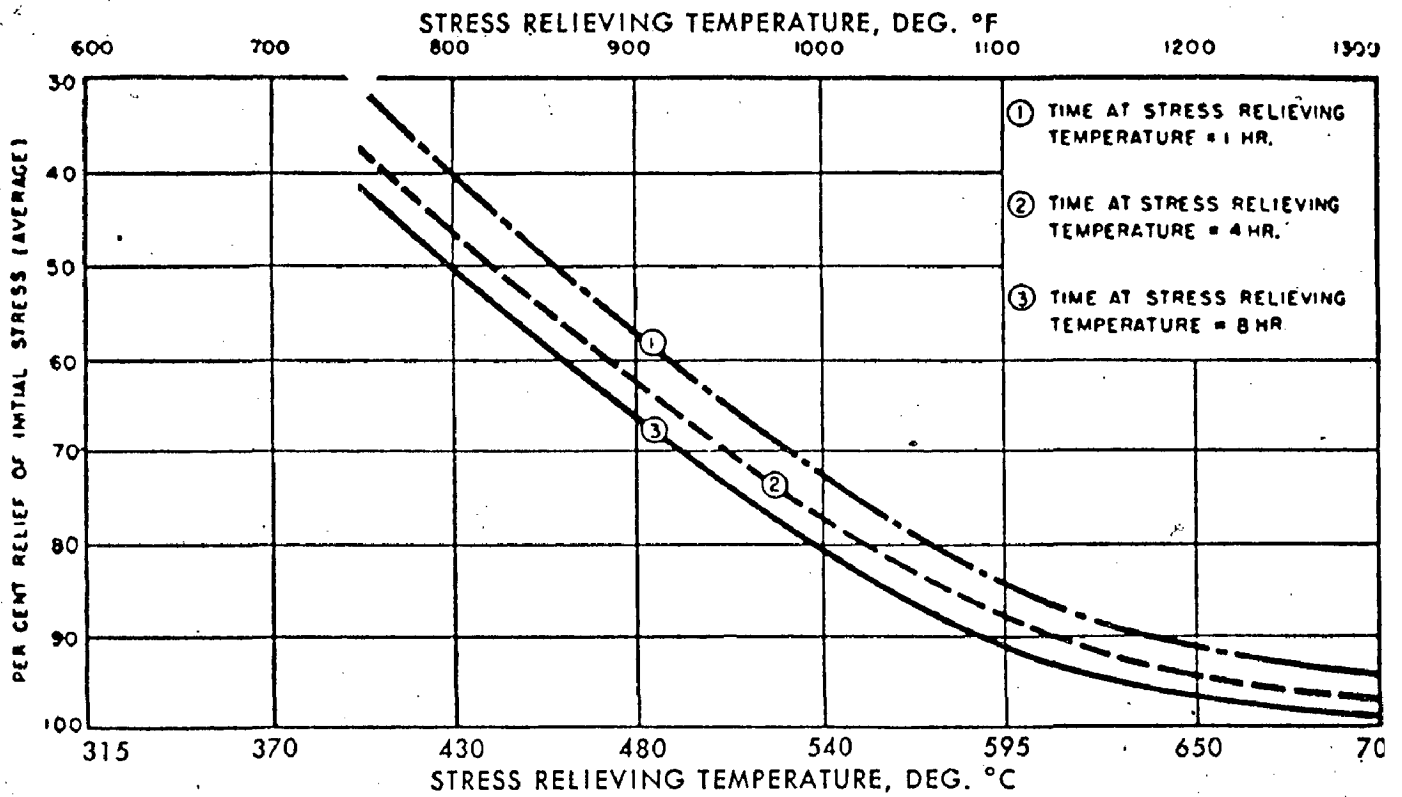


FIG. 2.5

EFFECT OF TEMP AND TIME ON STRESS RELIEF

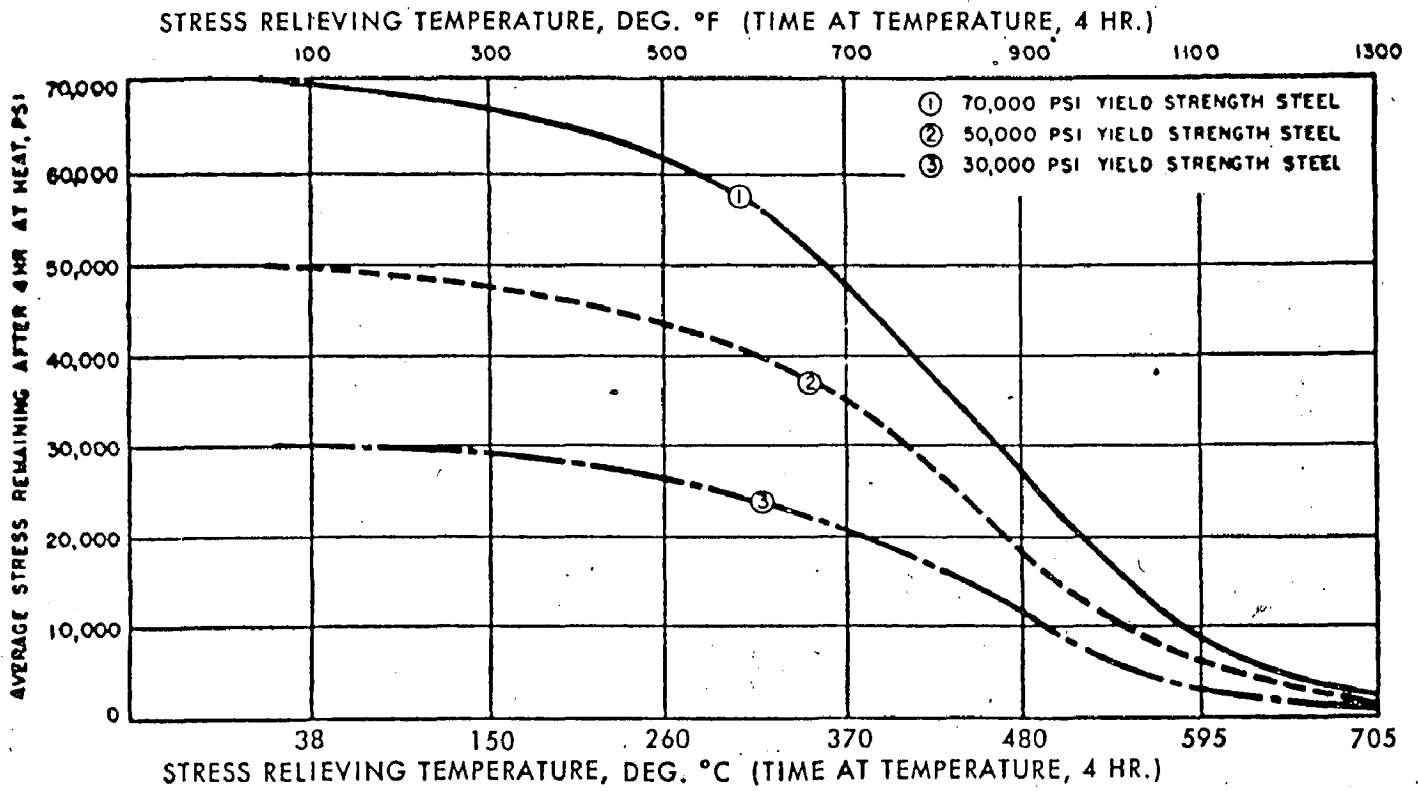


Fig. 2.6 —Effect of temperature and time on stress relief

1. *peak temp. in HAZ*
2. *estimating the width of HAZ*
3. *effect of preheat on the width of HAZ at y=0, $T_p=T_m$ hence peak temp. at the fusion boundary equals the melting point.*

Width of heat affected zone is directly proportional to the net energy input. Preheating also increases the width of heat affected zone. For several passes in the thick plates the cooling rate R of the weld and HAZ at a temperature T_c is given by $R = \frac{2\pi K(T_c - T_o)}{h(\text{net})}$, K is the thermal conductivity of the metal T_o is the initial plate temperature. From this equation it is clear that by increasing the preheat temperature of base metal cooling rate in weld and HAZ is reduced. Preheat for this purpose is often used for welding of hardenable steels.

The solidification time St (in seconds) of weld metal depends upon the net energy input and is expressed by the equation

$$St = \frac{Lh(\text{net})}{2\pi K C (T_m - T_o)^2}$$

where L = latent heat of fusion (J/mm^3)

Solidification time directly affects the structure of weld metal. Most alloys freeze dendritically. An important structural feature of weld metal is dendritic spacing. Dendritic spacing is proportional to the square root of solidification time. Larger energy input produces coarser structure. Dendritic structure directly influences the properties and response to heat treatment of weld. With most metals ductility and toughness improve with finer dendritic

spacing. Fine dendritic structure favours rapid response to heat treatment. Metallurgical considerations favour low arc energy input in which the extent of heat affected zone is minimized and weld metal properties are enhanced through production of fine dendritic structure. This reasoning favours the use of many small than a few large passes to produce a weld. In practical terms there are definite metallurgical benefits to be gained from the selection of stringer bead techniques. Fig 2.7 shows the typical thermal cycles produced in 13 mm steel plate by an arc weld made using an energy input of 3940 J/mm with an initial plate temperature of 27 °C. The following three features are evident from this figure.

1. The peak temperature decreases rapidly with increasing distance from the weld center line.
2. The time required to reach the peak temperature increases with increasing distance from the weld center line.
3. The rate of heating and the rate of cooling both decreases with increasing distance from the weld center line.

Fig. 2.8 illustrates the effect of energy input and preheat temperature on peak temperature distribution in HAZ for 13 mm thick shielded metal arc welded steel plate. Following three features are evident from this figure.

1. Decreasing either energy input or the preheat temp. provides a steeper distribution of peak temp. in the weld heat affected zone
2. Increasing the energy input causes a significant increase in the distance from the weld center line to a point exercising a particular peak temp. for all values of peak temperature.

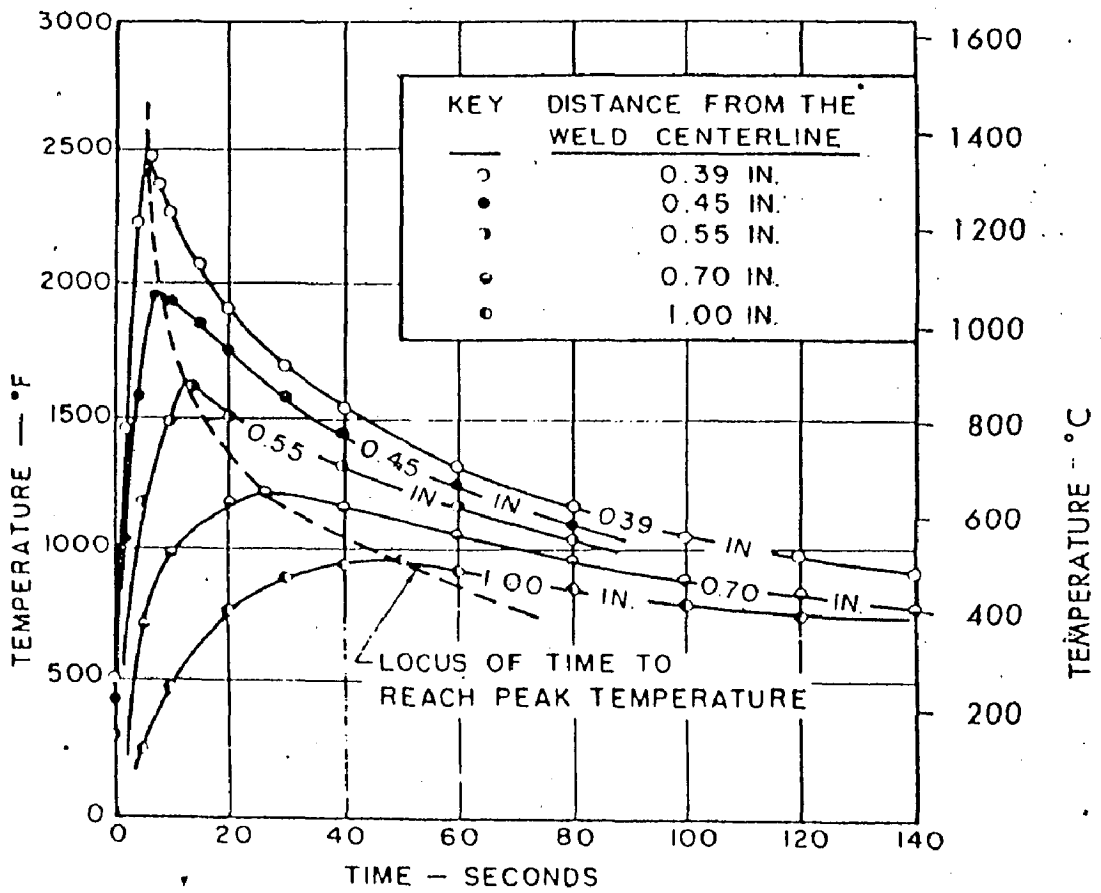


Fig. 2.7.—Thermal cycles experienced by indicated locations in the heat-affected zone of an arc weld made with 100,000 joules/in. for ½ in. steel plate at room temperature

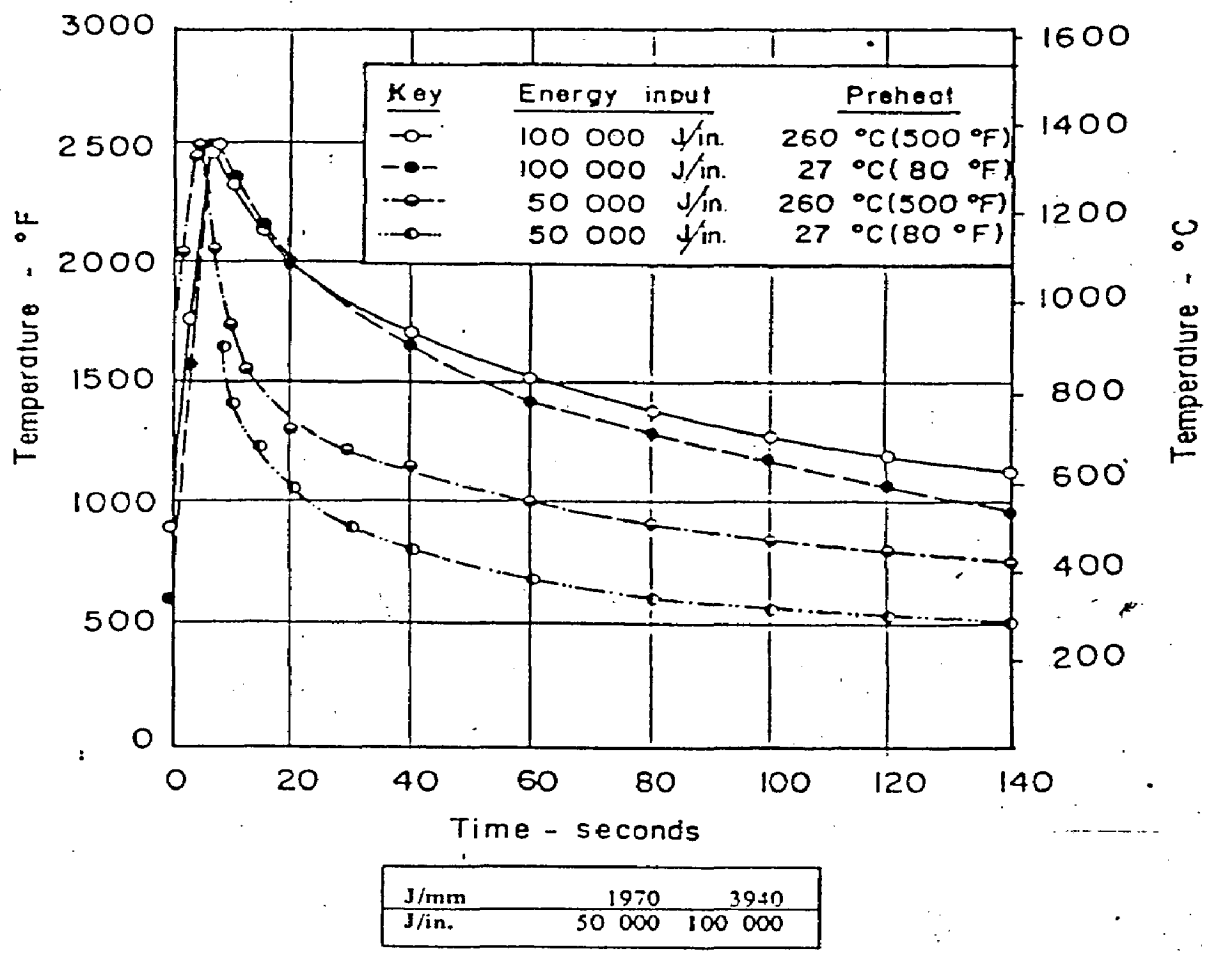


Fig 2.8—Effect of initial plate temperature on thermal cycles in the heat-affected zone of arc welds.

3. Increasing the preheat temperature increases the distance from the weld center line to a point experiencing a particular peak temperature by an amount that varies inversely with the value of peak temperature.

Fig. 2.9 summarizes the effect of energy input and preheat temperature on the actual weld thermal cycles in HAZ of arc welds in 13 mm thick plate. Locations are chosen to have a peak temperature of 1365°C. Corresponding points are at different locations from weld center line. Following is true for peak temperatures near the liquidus. For a given preheat temperature, increasing the energy input causes an increase in the time of exposure to temperature near the peak temperature and causes a decrease in cooling rate. For a given energy input, increasing the preheat temperature decreases the cooling rate but does not significantly increase the time of exposure to temperature near peak temperature.

2.7 DISTORTION AND RESIDUAL STRESSES

Distortion in weldments occurs from the non uniform contraction of the weld metal and expansion and contraction of adjacent base metal during the heating and cooling cycle of the welding process. As the temperature of weld area increases, Y_S , modulus of elasticity and thermal conductivity decrease and coefficient of thermal expansion and specific heat increase. These changes affect heat flow and uniformity of heat distribution. These variables make the precise calculation of changes during heating and cooling difficult. As the weld metal solidifies and fuses with the parent metal, it is in the maximum expanded state, it occupies the maximum possible volume as a solid. On cooling it tends to contract to the volume it would normally occur at lower temperature, but it is restrained from doing so

stresses that exceed YS of the weld are relieved by this accommodation. By the time the weld reaches the room-temperature assuming complete restraint of the base metal so that it cannot move, weld will contain locked in tensile stresses approximately equal to the YS of the metal. If the restraints are removed the locked in stresses are partially relieved, as they cause the base metal to move, thus distorting the weldment. Shrinkage in the base metal, adjacent to the weld adds to the stresses that lead to the distortion. During welding, the base metal adjacent to the weld metal is heated almost to the melting point temperature of the base metal a few inches from the weld is substantially lower. This large temperature difference causes non-uniform expansion followed by base metal movement or distortion. Volume of adjacent base metal that contributes to distortion can be controlled somewhat by welding procedure. Higher welding speeds for example reduces the size of adjacent base metal zone that shrinks along with the weld metal. Shrinkage of the weld causes various types of distortion and dimensional changes. A butt weld between two pieces of plate by shrinking transverse changes the width of assembly fig 2.10. It also causes angular distortion fig 2.11. Here the greater amount of weld metal and heat at the top of the joint produces greater shrinkage at the top causing the edges of the plates to be lifted. Longitudinal shrinkage of the same weld would tend to deform the joint plate as shown in fig 2.12. Angular distortion is also a problem with fillet welds. Refer fig 2.13 and 2.14.

Shrinkage Control :

Shrinkage cannot be prevented but it can be controlled.

1. Do Not Over Weld: The more metal placed in a joint, the greater is the shrinkage. Correctly sizing a weld for service requirement of the joint not only minimizes distortion but also saves weld metal and time.

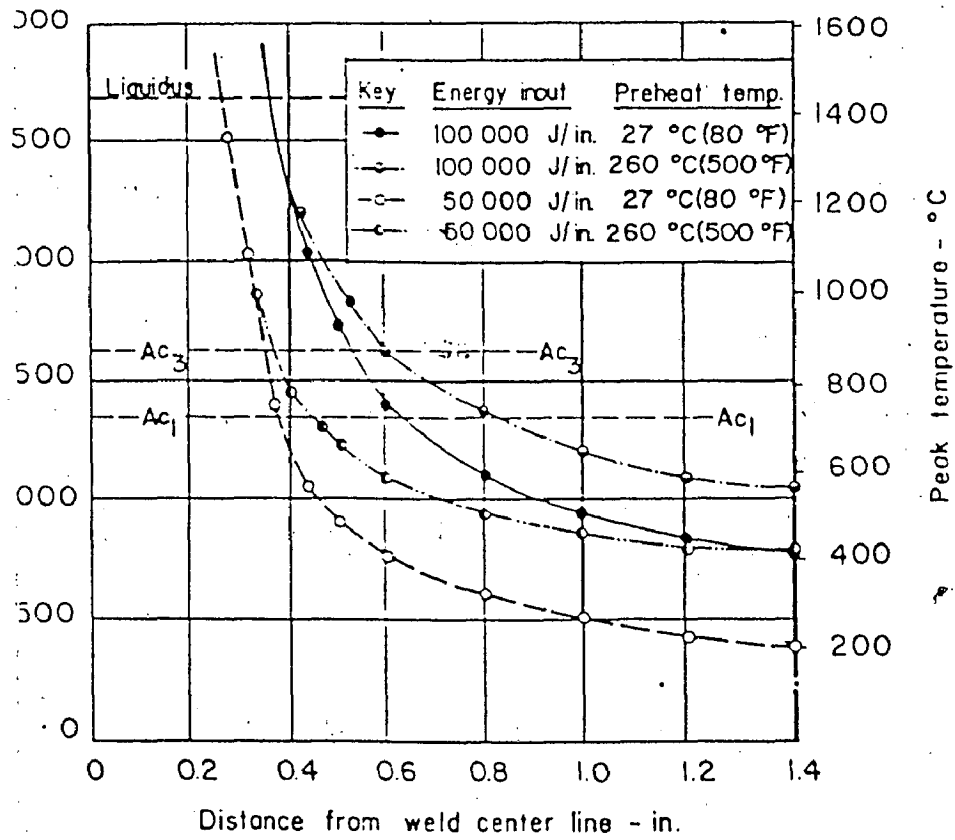


FIG 2.9 EFFECT OF INITIAL PLATE TEMP ON THERMAL CYCLE

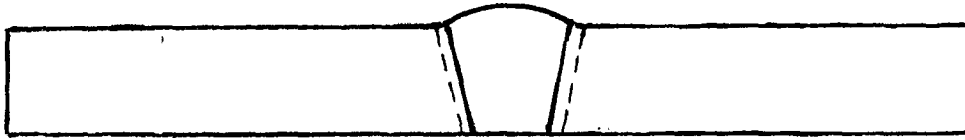


FIG 2.10 TRANSVERSE SHRINKAGE

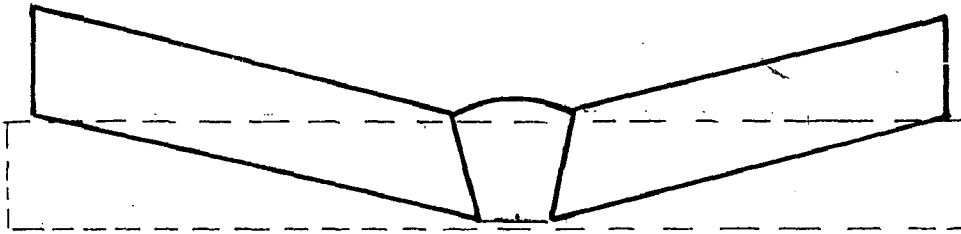


FIG 2.11 ANGULAR DISTORTION

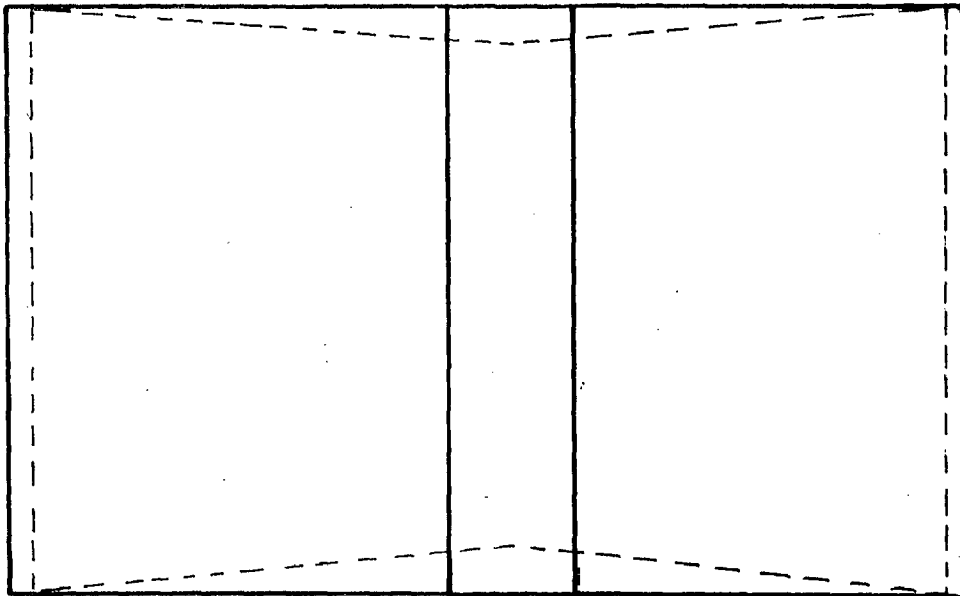


FIG 2.12 LONGITUDINAL SHRINKAGE

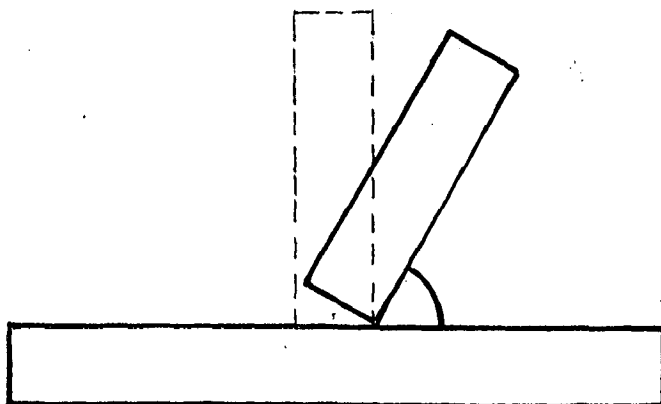
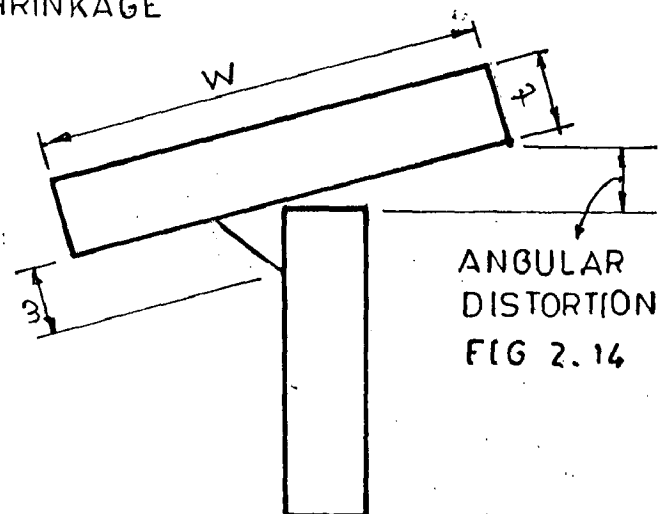


FIG 2.13 ANGULAR DISTORTION IN FILLET WELD



1. Do Not Over Weld: The more metal placed in a joint, the greater is the shrinkage. Correctly sizing a weld for service requirement of the joint not only minimizes distortion but also saves weld metal and time.

2. Use Intermittent Welding :

3. Use As Few Weld Passes As Possible : Fewer passes with bigger diameter electrodes are preferred to greater number of passes with small diameter electrode when transverse distortion is a problem

4. Use back step welding .

5. Plan the welding sequence.

6. Remove Shrinkage Forces After Welding: By peening. Root bead should never be peened, because of the danger of concealing a crack or causing one. Generally the peening is not permitted on final runs because of the possibility of covering a crack and interfering with inspection.

7. Minimize Welding Time : Since complex cycle of heating and cooling takes time, time factor affects distortion. It is desirable to finish the weld quickly before large volume of adjacent parent metal is heated up.

Transverse Shrinkage = $0.10 A/t$

Where A is the cross-section area of the weld. t is the weld thickness.

Angular distortion = $0.02 \frac{W}{t^2}$ fig 2.12

Where W = Flange width

w = Weld size

t = Flange thickness [13]

Residual Stress:

Stresses are induced by the unequal contraction of the filler metal and by the unequal expansion and contraction of HAZ during welding. Metal that has remained relatively cool during welding resists the contraction of the cooling weld metal. This causes the weld metal to stretch and thus causing opposite strains in the weldment. Opposite strains produce a system of stresses locked up in the weldment. In every welding process with the possible exception of friction welding and flash welding a large part of weld joint has time to cool before joint is completed. This circumstance obviously provides high degree of restraint. This factor indicates that high residual stresses exists irrespective of an external restraint. Residual stresses compose an internal force system that must be in equilibrium. If this was not the case some local point would be overstressed by simple addition of like forces when the system was subjected to externally applied loads. Externally applied loading in tension cannot be additive to residual stresses of like sign until the balancing compressive stresses to the system in equilibrium are overcome. Residual stresses have no detrimental effect on the static load properties of the weldments. These stresses could be harmful in cases where extreme rigidity exists so that no plastic flow could occur particularly in presence of a notch or stress raiser of some kind. If notches are present residual stresses should be removed from structures that will be subjected to impact load. Under conditions of repeated loading, residual stresses appear to have little effect on endurance strength if notches are absent. Residual tensile stresses of yield point magnitude exists in longitudinal direction in all welds over 18 inch in length, balanced by wide

bands of relatively low compressive stresses on each side of the weld. Fig 2.15.

Proportionally lower residual stresses exist in shorter weld unless conditions of unusual longitudinal restraint are present. An improvement has been established in the performance of welded structure made from notch sensitive steels as a result of thermal treatment.

2.8 COST OF REPAIRING

Labour, material, overhead and profit constitute Repair cost. Repair cost can be controlled by following factors:

Designing Welds: Use weld designs that require least weld metal. Welds should be placed at the most accessible location.

Conservation of material: Setting up fixtures.

Positions: Weld should be made in a position that is easiest to weld and faster.

Size and type of filler metal: Use correct size of wire, when using covered electrode burn them to short stub of ½" to 2".

Electrode cost increases in proportion to the stub length. In addition to this operator cost also increases 3% with each 2" of stub end size above the standard 2". Factors that can be taken into account for calculation of repair cost are following:

1. Non destructive tests for location of defects.

2. Excavation and removal of defects.
3. Further NDT to establish sound material.
4. Application of preheat (if necessary).
5. Welding of excavated areas.
6. NDT of repaired area.
7. Post weld heat treatment.

These stages can be upto 10 times the cost of the original welding operation.

Other costly unknowns associated with weld repairs include:

- a) handling operations
- b) shop floor space
- c) storage
- d) supervising cost
- e) down time cost on men and equipments
- f) delayed deliveries incurring penalty costs.

These refers to single stage repairs and consequently build up if the repair is not correct first time. Repair welding cost decreases to stable level as the productivity of the welding processes increases. There may be a cross over point where welding will be cheaper than renewal. Machining and heat treatment cost remains constant for a given process but can vary from process to process. Welding cost expressed in terms of cost/kg of weld deposit includes wages, consumables, machine and energy cost. Machine and energy cost are relatively small. A simplified equation for determining welding cost is as given below.

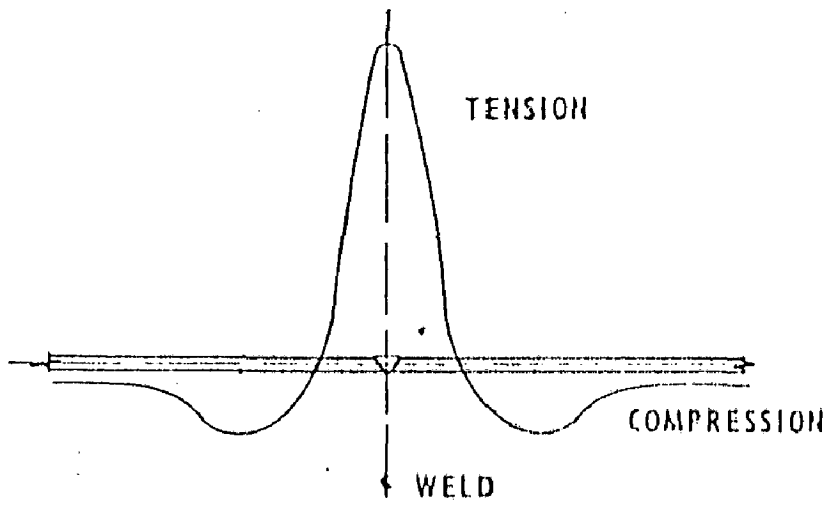


Fig. 2-15.—Distribution of longitudinal stresses

$$T = \frac{W}{HZ} + \frac{P_c}{N} + P \cdot f$$

where T = Total cost of weld deposit/kg.

W = Wages + overhead cost/hr.

H = Deposit rate in kg/hr.

Z = arc time factor.

P_c = Price of welding consumables cost/kg

P = Price of flux cost/kg.

f = Specific flux consumption.

N = efficiency.

Main factors that can be altered for a given process are the deposition rate and the arc time factor. Larger these two are, the lower the total cost. Cost of consumables is the limiting factor.

CHAPTER - 3

EXPERIMENTATION

3.1 BASE MATERIAL

In this investigation, the base material used was normalised and tempered forged C-Mn steel sections cut out in dimension of 300 mm dia and 20 mm thickness of two round shaft forgings, as schematically shown in Fig. 3.1. Chemical analysis of the plates was carried out on atomic absorption spectrometer and found as shown in table 3.1. Mechanical properties of the base material collected from both the shaft forgings were tested as given in table 3.2.

3.2 FILLER METAL

Supratherme (special) electrodes of the diameters 3.15 and 5 mm (specification AWS/ASME, SFA5.5 - E7018-1) were used. It is manufactured by M/s D&H Secheron electrodes pvt. ltd. Indore, India. The chemical composition of the electrodes was found as per table 3.3.

3.3 WELDING EQUIPMENT

The welds were made by shielded metal arc welding process using direct current electrode positive (DCEP) technique. A constant current characteristics welding rectifier whose specifications are given below was used as the power source for welding.

Welding Power Source Specification :

Make : Advani Oerlikon Model GL 500/600.

Range : 50-600 amps, 3 phase, 50 Hz frequency.

Input power 60% duty cycle : 41.8 kVA.

Current 60% duty cycle : 550 amps.

Cooling : forced air.

Welding electrode size : 2-6.3 mm

3.4 WELDING OF PLATES

3.4.1. Edge Preparation

V-groove edge preparation with root face and V angle, schematically shown in Fig 3.1 was made in the plates by air arc gouging, followed by grinding. For gouging dia 12 mm electrodes were used at a current of 500 amps and air pressure of 8 kg/cm². Before air arc gouging the plates were locally preheated using LPG burners to a temperature of 150 °C.

3.4.2. NDT of plates

After edge preparation the weld plates were examined by magnetic particle test and ultrasonic test to ensure absence of any flaws in the plates. Magnetic particle test was carried out by DC Yoke with a lifting power of 18 kg. For Ultrasonic test, Kraut Krammer Germany make USM-3S equipment was used. Probes used were 2 MHz normal beam (B2SE) and twin crystal probe (SEB2E).

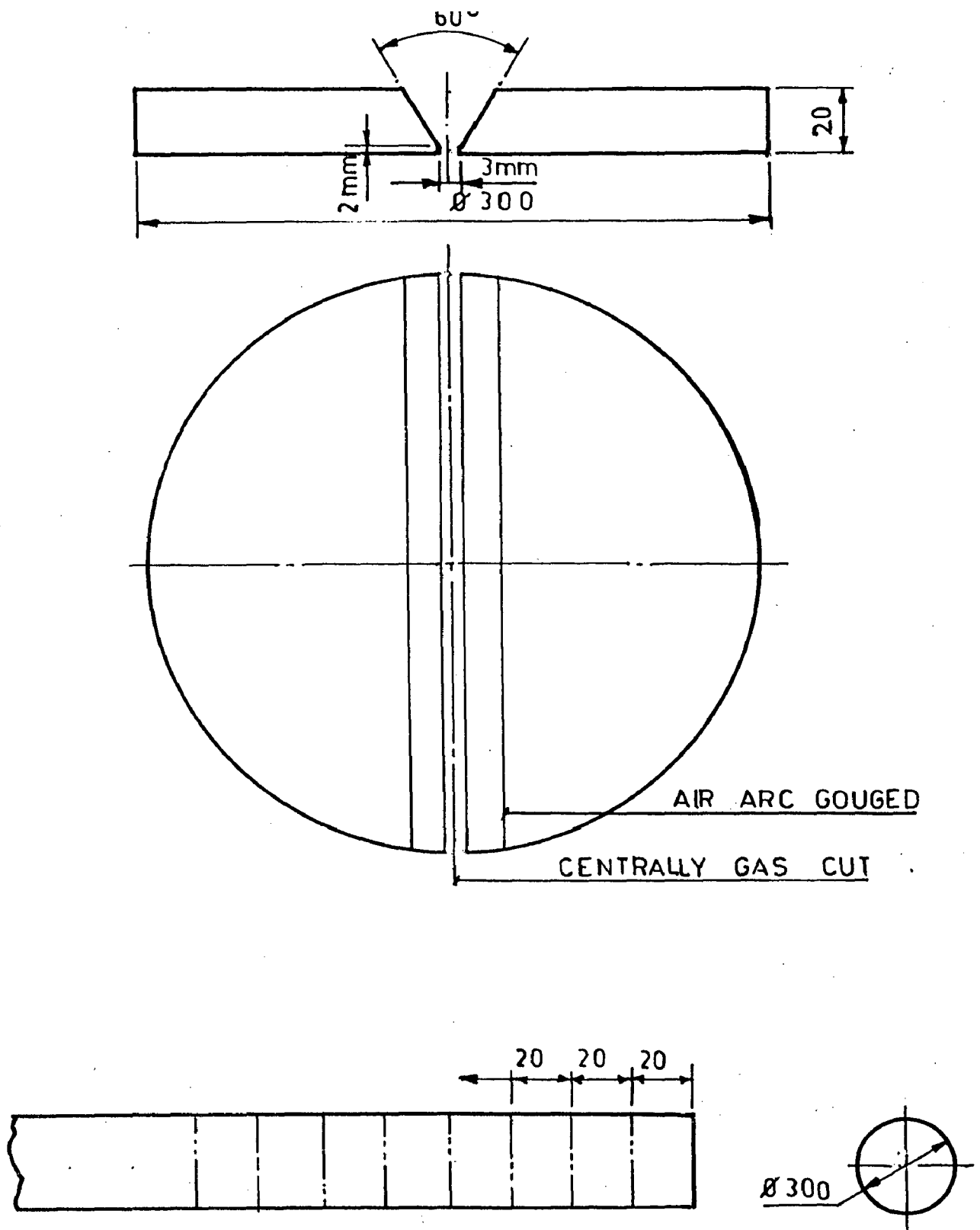


FIG 3.1 SCHEMATIC DIAGRAM FOR COLLECTION OF PLATES AND
EDGE PREPARATION ON PLATES

3.4.3. Welding

Prior to welding, the plates were thoroughly cleaned so as to remove any dirt or grease especially adhering to the groove surface of the plates. Welding of the plates was carried out at parameters as given in table 3.4. Welding of the forged plates was carried out using a fixture as shown in figure 3.2. After welding from the top the strong back up was removed and again welded to the other side of the weld joint followed by back gouging and grinding of the gouged area. Before filling this area by welding, it was assured by dye penetrant (D.P.) test that no surface crack is present in this area. (Welding was carried out at three different levels of preheat temperatures such as 100, 150 and 250 C. At each preheat level two plates were welded with 3.15 mm electrodes and two plates were welded with 5.00 mm electrodes. Welded plates were designated as given in table 3.4).

For the preparation of weld joints designated as A,B, and C, plates from shaft forging (2) were used and for preparation of weld joints designated as D, E, and F the plates for shaft forging (1) were used.

3.4.4. NDT of welded plates

After completion of welding, the weld and adjoining regions were examined by magnetic particle test using DC yokes and ultrasonic test using normal beam, receiver transmitter and angle beam (45°) probes, confirming the presence of no defect in the weld joint.

3.4.5. Post weld heat treatment

From the two welds prepared at preheat level and electrode size, one plate was post weld heat treated at 510 °C for 5 hrs and the other at 510 °C for 10 hrs. The temperature for post weld heat treatment was selected on the basis of last tempering operation of the shaft forgings i.e, 530 °C. As per AWS norms the recommended holding time at 510 °C is 10 hrs minimum. Considering the industrial applications of 10 hrs holding time, a comparatively shorter period of stress relieving for 5 hrs. have also been tried to study the effect of reduced soaking time on mechanical properties and fatigue strength of the welded joint.

3.5 MECHANICAL TESTING

3.5.1. Specimen collection

The run on and the run off portion of the welded plates were discarded to avoid incomplete penetration of the starting due to cold start and crater formation at the end of the weld. The tensile and fatigue test specimens were collected from the transverse section of the welded plate as schematically shown in fig. 3.3. Specimen for tensile and fatigue were prepared by removing the reinforced bead portion as well as base metal upto a depth of 2 mm from both the sides of the plates as shown in figure 3.4. The specimens were then prepared according to standard ASTM practice. The schematic diagrams of tensile and fatigue test specimens are shown in figure 3.5 and 3.6 respectively.

3.5.2 Tensile Test

Tensile testing of specimens was carried out on Mohr and Feder Half 6 Ton universal testing machine, pulsator type having a maximum load capacity of 6 Ton in static and 4 Ton in dynamic condition. The tensile

TABLE 3.4

WELDING PARAMETERS AND SPECIMEN DESIGNATION

| PREHEAT | ELECTRODE SIZE | WELDING CURRENT | ARC VOLTAGE | TRAVEL SPEED | WELD DESIGNATION |
|---------|----------------|-----------------|-------------|--------------|------------------|
| (°C) | (mm) | (Amp) | (Volts) | (cm/min) | |
| 100 | ∅5.00 | 200 | 24 | 18 | A1 A2 |
| 150 | ∅5.00 | 200 | 24 | 18 | B1 B2 |
| 250 | ∅5.00 | 200 | 24 | 18 | C1 C2 |
| 100 | ∅3.15 | 110 | 24 | 18 | D1 D2 |
| 150 | ∅3.15 | 110 | 24 | 18 | E1 E2 |
| 250 | ∅3.15 | 110 | 24 | 18 | F1 F2 |

TABLE 3.1

CHEMICAL COMPOSITION OF BASE MATERIAL

| ALLOYING ELEMENTS | COMPOSITION (WT%) | |
|----------------------|-------------------|-------------------|
| | SHAFT FORGING (1) | SHAFT FORGING (2) |
| C | 0.17 | 0.18 |
| S | 0.024 | 0.021 |
| P | 0.019 | 0.027 |
| Si | 0.300 | 0.200 |
| Mn | 1.350 | 1.480 |
| Ni | 0.160 | 0.300 |
| Cr | 0.150 | 0.200 |
| Mo | 0.100 | 0.140 |

247837

TABLE 3.2

MECHANICAL PROPERTIES OF BASE MATERIAL

| PROPERTIES | SHAFT FORGING (1) | SHAFT FORGING (2) |
|--------------------------|------------------------------|------------------------------|
| YS (N/mm ²) | 323 | 358 |
| UTS (N/mm ²) | 517 | 546 |
| % El (l=5d) | 21.2 | 27.2 |
| % R.A. | 33.8 | 56.2 |
| HARDNESS (BHN) | 148-151 | 161-170 |

TABLE 3.3

CHEMICAL COMPOSITION OF FILLER METAL

| DIA OF ELECTRODE | CHEMICAL COMPOSITION (WT%) | | | | | | | |
|-------------------------|-----------------------------------|--------------|--------------|-------------|-------------|---------------|---------------|---------------|
| | C | S | P | Si | Mn | Ni | Cr | Mo |
| 3.15 | 0.06 | 0.019 | 0.021 | 0.37 | 1.55 | Traces | Traces | Traces |
| 5.00 | 0.06 | 0.014 | 0.020 | 0.42 | 1.47 | 0.05 | Traces | 0.080 |

3.4.3. Welding

Prior to welding, the plates were thoroughly cleaned so as to remove any dirt or grease especially adhering to the groove surface of the plates. Welding of the plates was carried out at parameters as given in table 3.4. Welding of the forged plates was carried out using a fixture as shown in figure 3.2. After welding from the top the strong back up was removed and again welded to the other side of the weld joint followed by back gouging and grinding of the gouged area. Before filling this area by welding, it was assured by dye penetrant (D.P.) test that no surface crack is present in this area. (Welding was carried out at three different levels of preheat temperatures such as 100, 150 and 250 C. At each preheat level two plates were welded with 3.15 mm electrodes and two plates were welded with 5.00 mm electrodes. Welded plates were designated as given in table 3.4).

For the preparation of weld joints designated as A,B, and C, plates from shaft forging (2) were used and for preparation of weld joints designated as D,.E, and F the plates for shaft forging (1) were used.

3.4.4. NDT of welded plates

After completion of welding, the weld and adjoining regions were examined by magnetic particle test using DC yokes and ultrasonic test using normal beam, receiver transmitter and angle beam (45°) probes, confirming the presence of no defect in the weld joint.

3.4.5. Post weld heat treatment

From the two welds prepared at preheat level and electrode size, one plate was post weld heat treated at 510 °C for 5 hrs and the other at 510 °C for 10 hrs. The temperature for post weld heat treatment was selected on the basis of last tempering operation of the shaft forgings i.e, 530 °C. As per AWS norms the recommended holding time at 510 °C is 10 hrs minimum. Considering the industrial applications of 10 hrs holding time, a comparatively shorter period of stress relieving for 5 hrs. have also been tried to study the effect of reduced soaking time on mechanical properties and fatigue strength of the welded joint.

3.5 MECHANICAL TESTING

3.5.1. Specimen collection

The run on and the run off portion of the welded plates were discarded to avoid incomplete penetration of the starting due to cold start and crater formation at the end of the weld. The tensile and fatigue test specimens were collected from the transverse section of the welded plate as schematically shown in fig. 3.3. Specimen for tensile and fatigue were prepared by removing the reinforced bead portion as well as base metal upto a depth of 2 mm from both the sides of the plates as shown in figure 3.4. The specimens were then prepared according to standard ASTM practice. The schematic diagrams of tensile and fatigue test specimens are shown in figure 3.5 and 3.6 respectively.

3.5.2 Tensile Test

Tensile testing of specimens was carried out on Mohr and Feder Half 6 Ton universal testing machine, pulsator type having a maximum load capacity of 6 Ton in static and 4 Ton in dynamic condition. The tensile

TABLE 3.4

WELDING PARAMETERS AND SPECIMEN DESIGNATION

| PREHEAT | ELECTRODE SIZE | WELDING CURRENT | ARC VOLTAGE | TRAVEL SPEED | WELD DESIGNATION |
|---------|----------------|-----------------|-------------|--------------|------------------|
| (°C) | (mm) | (Amp) | (Volts) | (cm/min) | |
| 100 | ∅5.00 | 200 | 24 | 18 | A1 A2 |
| 150 | ∅5.00 | 200 | 24 | 18 | B1 B2 |
| 250 | ∅5.00 | 200 | 24 | 18 | C1 C2 |
| 100 | ∅3.15 | 110 | 24 | 18 | D1 D2 |
| 150 | ∅3.15 | 110 | 24 | 18 | E1 E2 |
| 250 | ∅3.15 | 110 | 24 | 18 | F1 F2 |

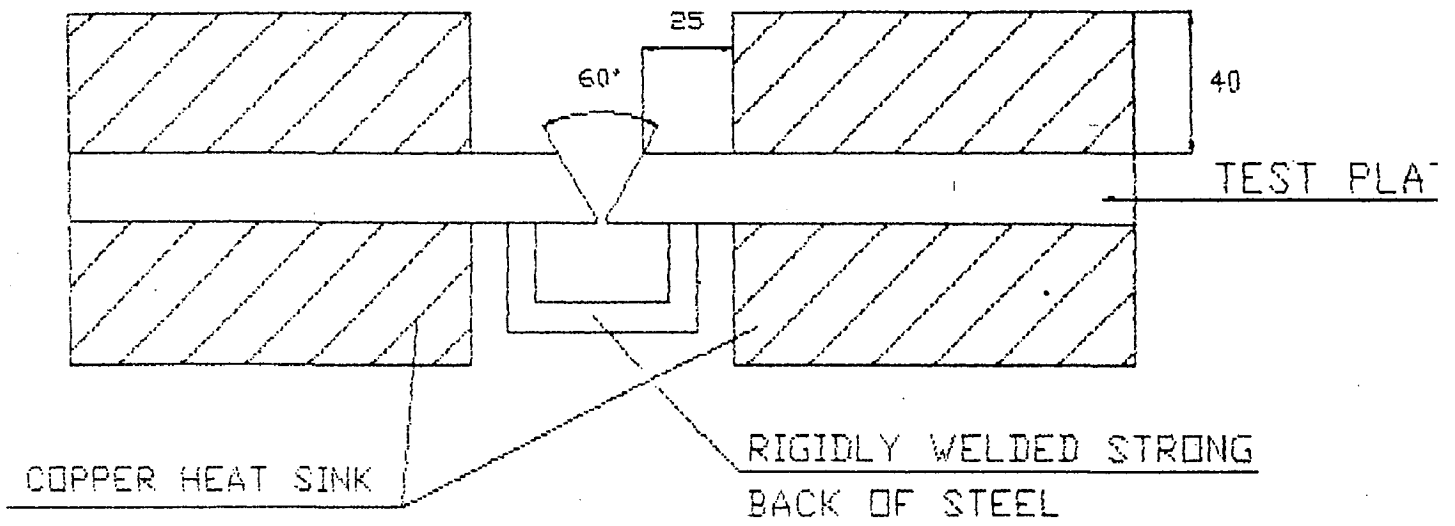


FIG 3.2 FIXTURE FOR WELDING OF PLATE

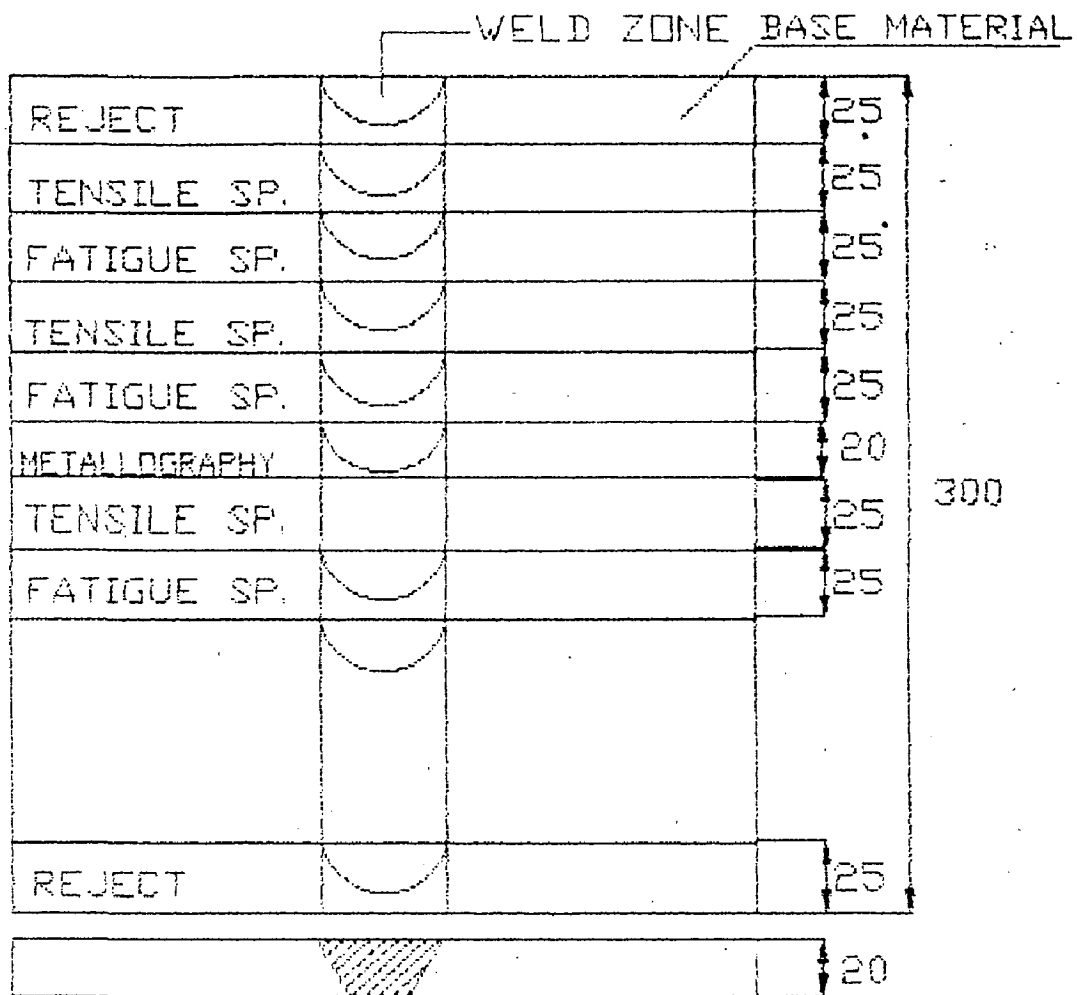


FIG 3.3 SECTIONING PLAN FOR PREPARATION OF SAMPLES

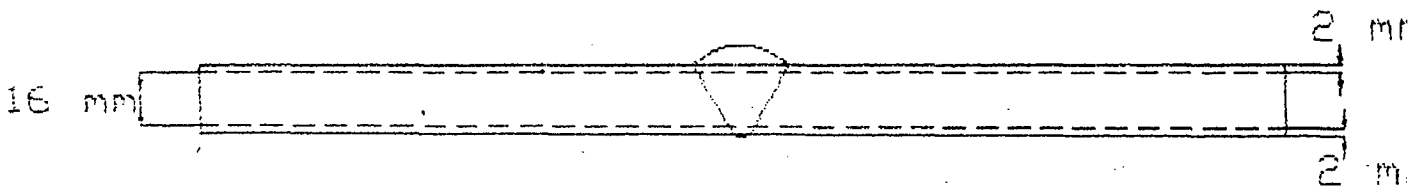


FIG 3.4 DIAGRAM SHOWING THE MACHINING THICKNESS
FROM BOTH SIDES FOR SPECIMEN FABRICATION

247837



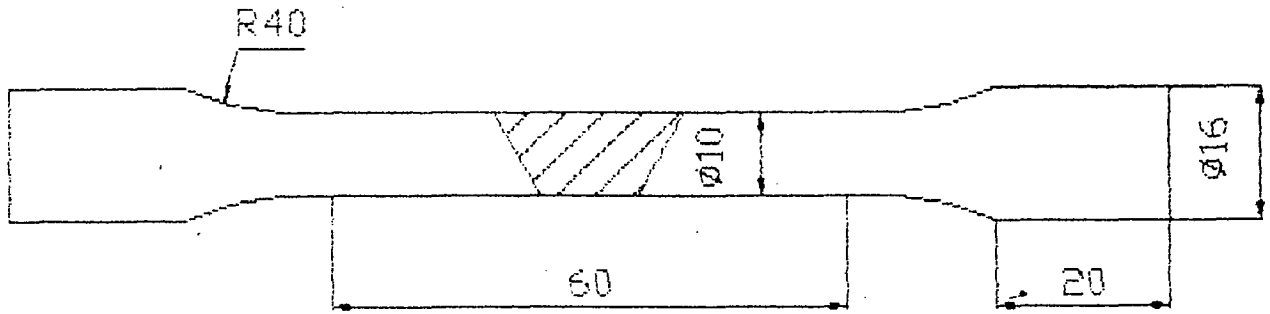


FIG 3.5 DIAGRAM SHOWING THE DIMENSIONS OF TENSILE SPECIMEN

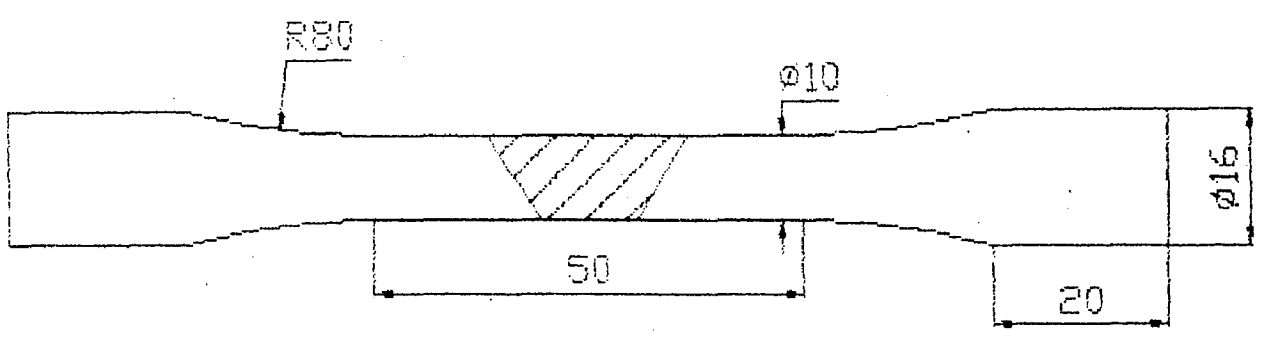


FIG 3.6 DIAGRAM SHOWING THE DIMENSIONS OF FATIGUE SPECIMEN

3.6 METALLOGRAPHY EXAMINATION

For metallographic examination, the specimens were collected from the central region of the welded plate. The specimens were cut into a suitable size of 50x20 mm from transverse section of the welded plates. Transverse section of the weld joint was prepared according to the standard metallographic procedure. The specimen was initially polished with various grades of emery paper 200, 320, 500, 800, 1000 and 1200 grade nos., from coarse to fine respectively. Then the specimens were polished by using polishing grade alumina powder on a polishing wheel having velvet cloth mounted on it. The polished specimens were etched by Nital reagent (HNO₃ 5 ml, Methanol 100 ml). The specimens were etched by dipping into ~~etchant~~ etchant for about 15-20 seconds, followed by washing with stream of water and then drying with cotton.

3.6.1. Optical metallography

The microstructure of weld deposit and HAZ were studied under optical microscope (Leitz Microscope mm 6) and photographed. Width of HAZ revealed in the matrix adjacent to fusion line was measured at number of places by positioning a micro scale inserted inside the eye piece perpendicular to the fusion line.

3.7. HARDNESS MEASUREMENT

The vickers hardness of heat affected zone was measured using a load of 5 kg on a Wolpert Hardness tester. The hardness measurement was carried out on transverse section of the etched specimen. The diagonal of the impressions were measured and from their mean value corresponding VHN was noted from a standard chart.

CHAPTER -4

RESULTS AND DISCUSSION

4.1 BASE MATERIAL PROPERTIES

4.1.1. Microstructure

The microstructures of base metals collected from two different shaft forgings are shown in figure 4.1. It is observed that both the shaft forgings are having microstructure consisting of ferrite and pearlite. However the shaft forging 2 is found to have comparatively more pearlite than the shaft forging 1, which is in agreement to the chemical composition of shaft forgings (table 3.1), showing the presence of comparatively higher amount of C content in shaft forging 2. Observed difference in chemical composition and microstructure can be taken as inherited variations present in the class of forgings arising out of variations in different commercial processing conditions.

4.1.2. Mechanical Properties

The inherited variations in chemical composition and microstructures of the shaft forgings as discussed above introduces a commonly observed variation in mechanical properties. Observed mechanical properties of two shaft forgings used in this investigation are shown in table 4.1. Table depicts that variation in UTS, YS and % elongation of shaft forgings are lying in the range of 5.6, 10.8 and 28% respectively.

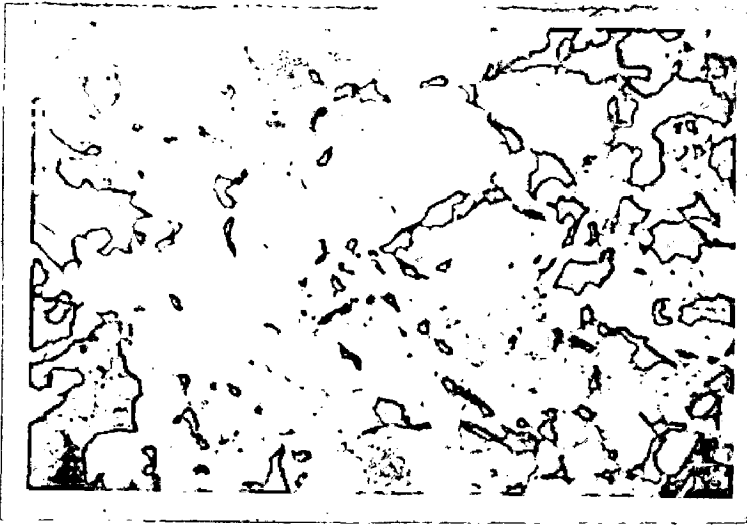
4.2 MICROSTRUCTURE OF WELD METAL

At a given electrode dia of 3.15 mm the effect of post weld heat treatment for 5 and 10 hrs at 510°C on the microstructure of weld deposits under three different preheating 100, 150 and 250°C are shown in figs 4.2 (a,b,c) and 4.3(a,b,c) respectively. Similarly at a given higher electrode diameter of 5.00 mm, the effect of post weld heat treatment for 5 and 10 hrs at 510°C on the microstructure of weld deposits under three different preheating are shown in figs 4.4(a,b,c) and 4.5(a,b,c) respectively. In this investigation, any effect of different electrode sizes and preheating on the microstructure of weld deposit is practically lost their identification due to post weld heat treatment at a high temperature of 510°C for different times.

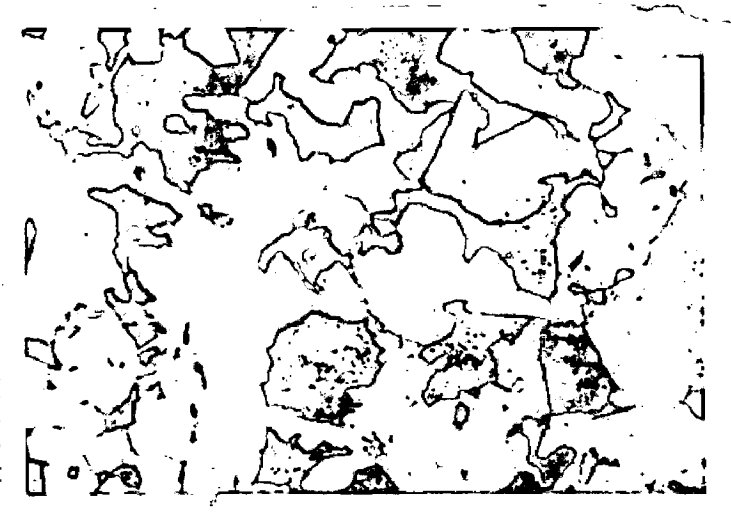
However a comparison of the microstructure presented in figs. 4.2 and 4.3 and also in figs. 4.4 and 4.5 clearly reveals that use of higher post weld heat treatment for longer time of 10 hrs at 510°C cause significant coarsening of grain size and pearlite colonies in the matrix.

4.3 MICROSTRUCTURE OF HAZ

The effect of welding using different sizes of electrodes at different preheating and post weld heat treatments on the width of HAZ has been shown in table 4.2 and figs. 4.6 & 4.7. This table shows that the width of HAZ is enhanced with the increase in preheating temperature from 100 to 250°C and with an increase in electrode size from 3.15 mm to 5.00 mm. This has happened due to the increase in heat input with the increase of electrode diameter and temperature of preheating. However it is marked that variation in post weld heat treatment does not have any significant influence on the width of HAZ. This behaviour infers that the width of HAZ is primarily dictated by welding conditions and not by the post weld heat treatments. At a given electrode diameter of 3.15 mm, the effect of post weld



SHAFT FORGING 1



SHAFT FORGING

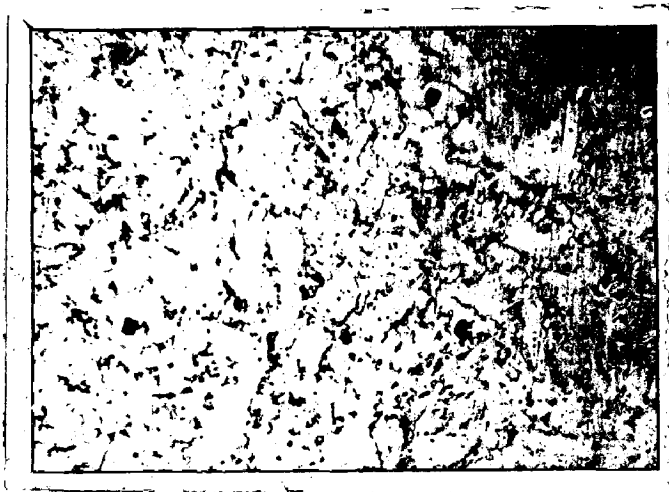
TABLE 4.1

MECHANICAL PROPERTIES OF BASE MATERIALS

| PROPERTIES | SHAFT FORGING(1) | SHAFT FORGING(2) |
|-------------------------|-------------------------|-------------------------|
| YS(N/mm ²) | 323 | 358 |
| UTS(N/mm ²) | 517 | 546 |
| %ELONGATION (l=5d) | 21.2 | 27.2 |
| %R.A. | 33.8 | 56.2 |
| HARDNESS(BHN) | 148-151 | 161-170 |



Preheat 100° C



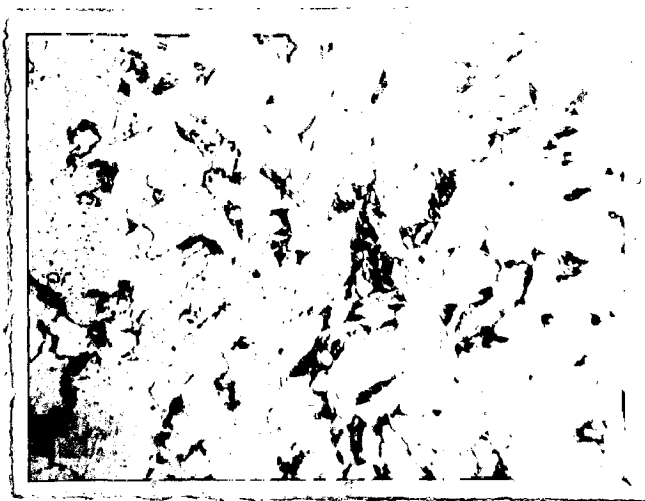
Preheat 150



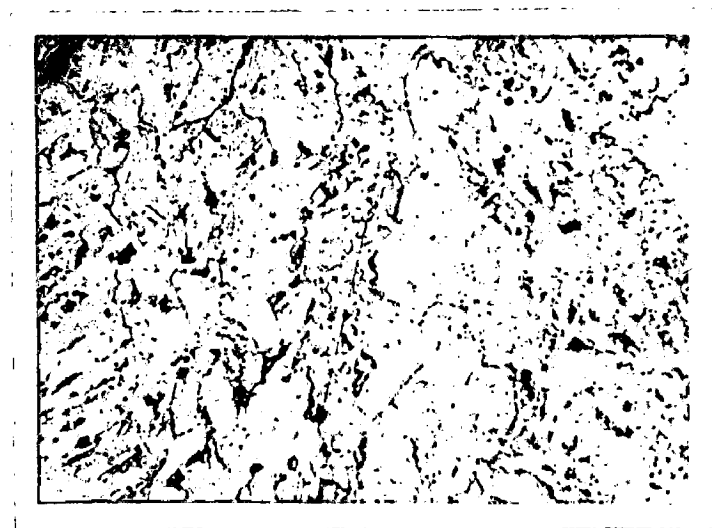
Preheat 250° C



Preheat 100° C

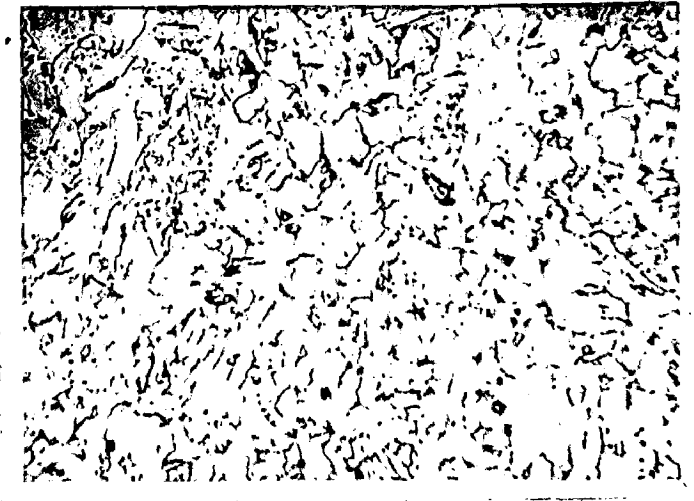


Preheat 150° C

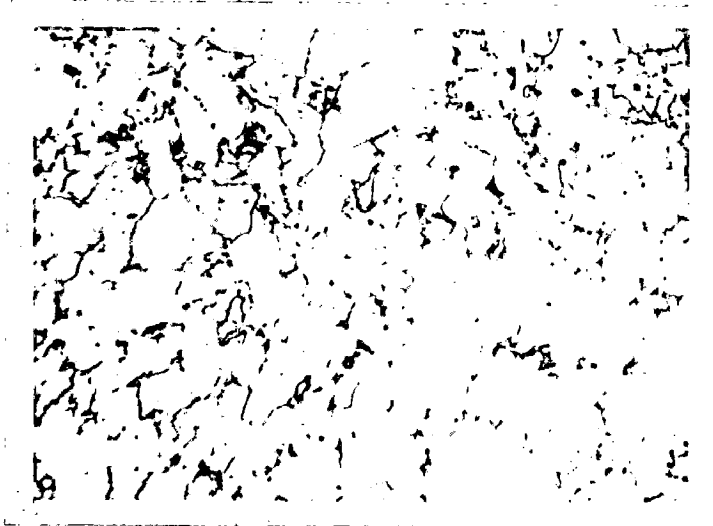


Preheat 250° C

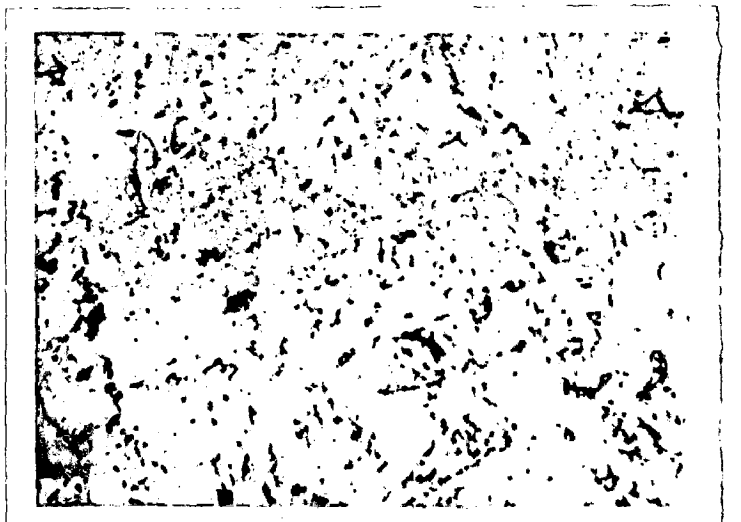
4.3(a,b,c) Micrographs at 200X showing the effect of preheating on the weld metal microstructures at a PWHT of 510° C 10 hrs using Ø2.15 mm electrodes



Preheat 100° C



Preheat 150° C



Preheat 250° C

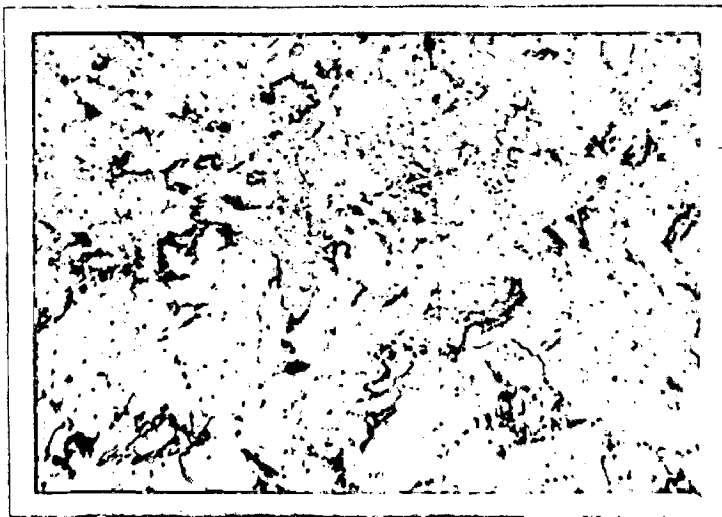
4.4(a,b,c) Micrographs at 200X showing the effect of preheating on the weld metal microstructures at a PWHT of 510° C. Electrodes: 25 00 mm electrodes



Preheat 100



Preheat 150° C



Preheat 250° C

4.5(a,b,c) Micrographs at 200X showing the effect of preheating on the weld metal microstructures at a PWHT of 510° C 10 hrs using Ø5.00 mm electrodes

TABLE 4.2 RESULTS OF MEASUREMENT OF WIDTH OF HAZ

| SPECIMEN NO. | MEAN WIDTH OF HAZ (mm) | STANDARD DEVIATION |
|--------------|------------------------|--------------------|
| D1 | 2.04 | 0.244 |
| D2 | 1.97 | 0.260 |
| E1 | 2.76 | 0.151 |
| E2 | 2.58 | 0.210 |
| F1 | 3.23 | 0.159 |
| F2 | 3.08 | 0.169 |
| A1 | 3.50 | 0.354 |
| A2 | 3.47 | 0.200 |
| B1 | 4.75 | 0.377 |
| B2 | 5.00 | 0.304 |
| C1 | 5.25 | 0.261 |
| C2 | 5.50 | 0.321 |

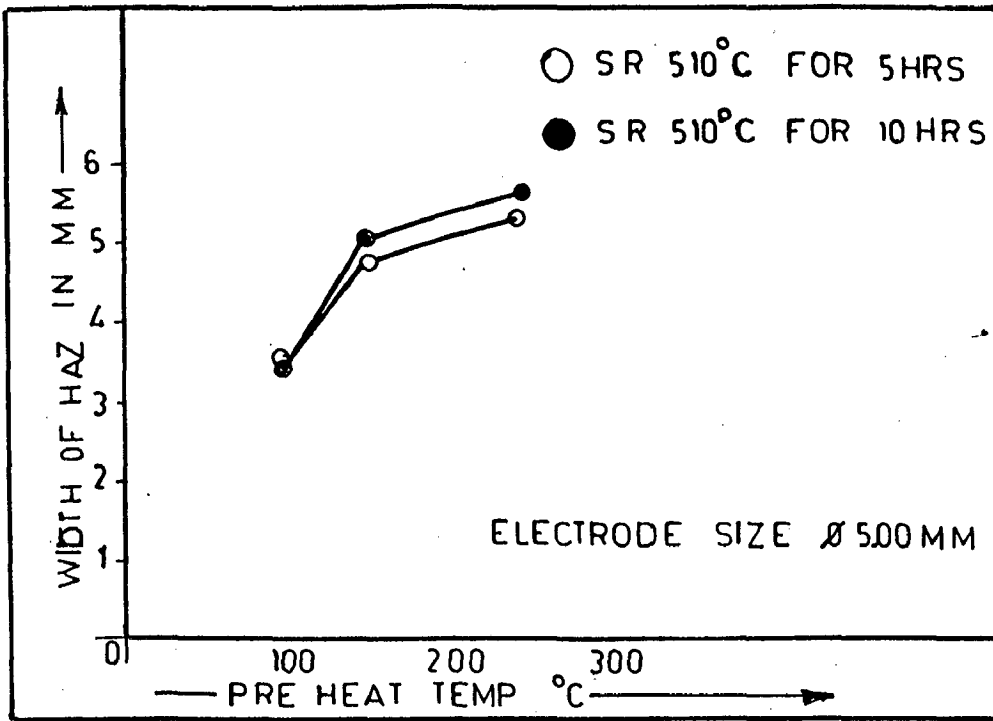


FIG 4.6 EFFECT OF PREHEAT TEMPERATURE ON THE WIDTH OF HAZ

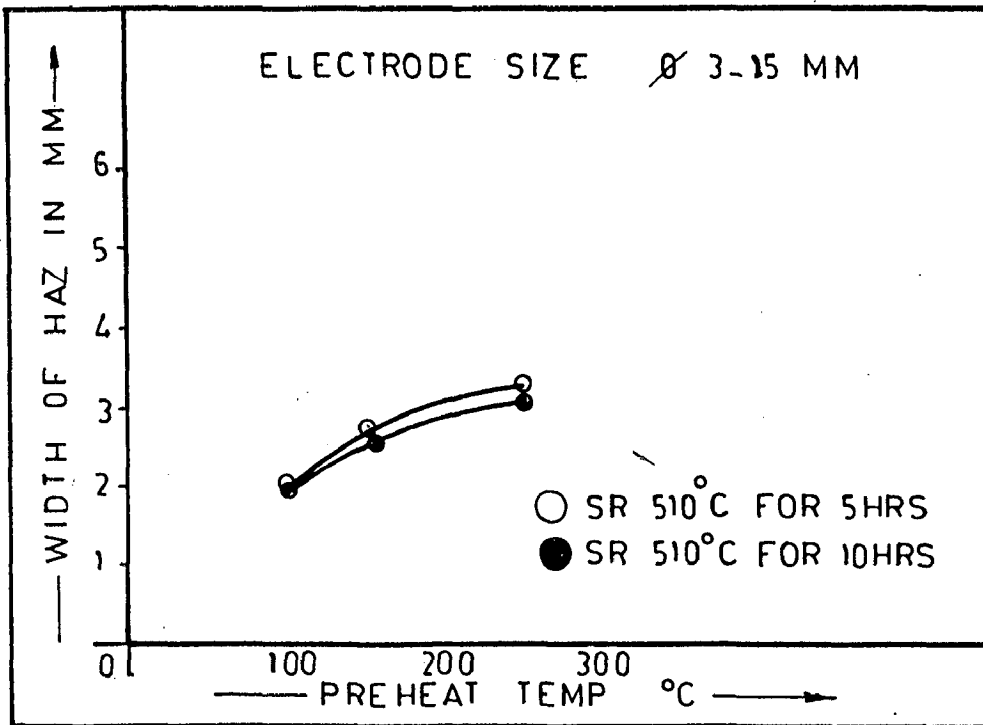


FIG 4.7 EFFECT OF PREHEAT TEMPERATURE ON THE WIDTH OF HAZ

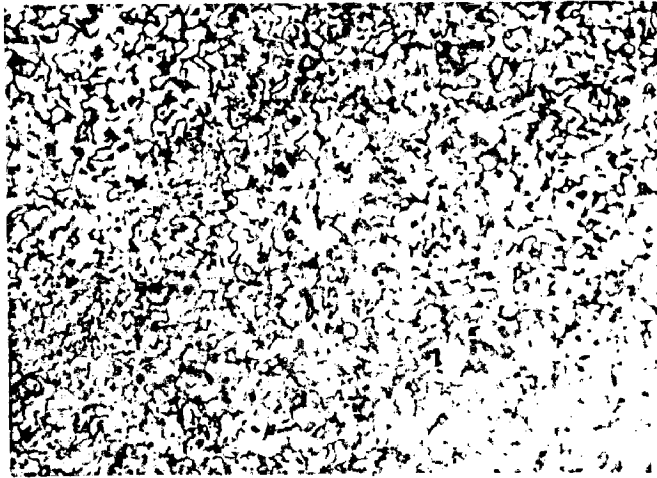
under different conditions of post welds heat treatment for 5 and 10 hrs at 510°C has been shown in fig 4.13. In both the figs. it is observed that increase in preheat temperature reduces the hardness of HAZ. The figs also show that at a given preheat temperature increase in post weld heat treatment time from 5 to 10 hrs at 510°C also marginally reduces the hardness of HAZ. But a comparison of figures 4.12 and 4.13 depicts that the use of higher diameter electrodes of $\phi 5.00$ mm comparatively enhances the hardness of HAZ with respect to that observed in case of welding with $\phi 3.15$ mm electrodes. The reduction in hardness of HAZ with increase in preheat temperature may be primarily attributed to increase in grain coarsening of HAZ during post weld heat treatment. This is possibly resulted from the presence of comparatively lower amount of martensite in case of higher preheating temperature, which pins down the grain coarsening.

4.5 TENSILE PROPERTIES OF WELD JOINTS

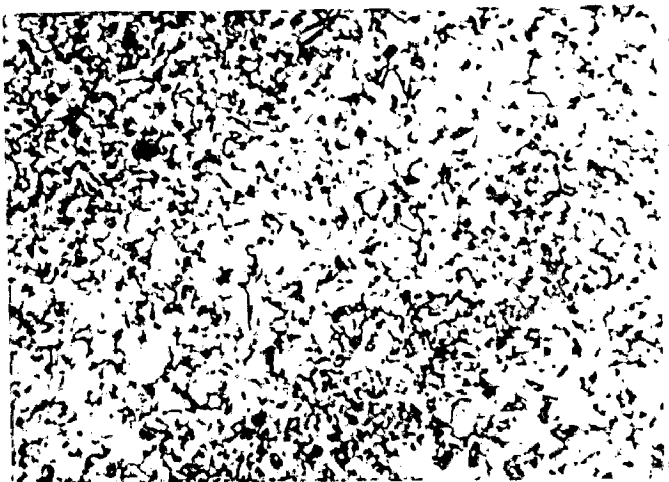
The typical behaviour of tensile load displacement curves of weld joints prepared by using $\phi 5.00$ and $\phi 3.15$ mm electrodes have been shown in fig 4.14(a & b) respectively. The curves have been shown in fig 4.14 (a & b) respectively. The curves have been found to clearly reveal the yield point of the material. During tensile test it was observed that weld joints produced by using $\phi 3.15$ mm electrodes were mostly found to fracture from weld centre (ref. fig 4.14b), whereas the weld joints prepared using $\phi 5.00$ mm electrodes always fractured from base metal, fig 4.14a. Thus it may be assumed that the yield point revealed in the curves shown in fig 4.14a represent the yield point of base material, but the yield point revealed in curves presented in fig 4.14b is represented by the yield point of weld deposit. The yield strength of the weld deposit has been marked under fig 4.14(b) as about 418.3 N/mm².



Preheat 100° C



Preheat 150° C

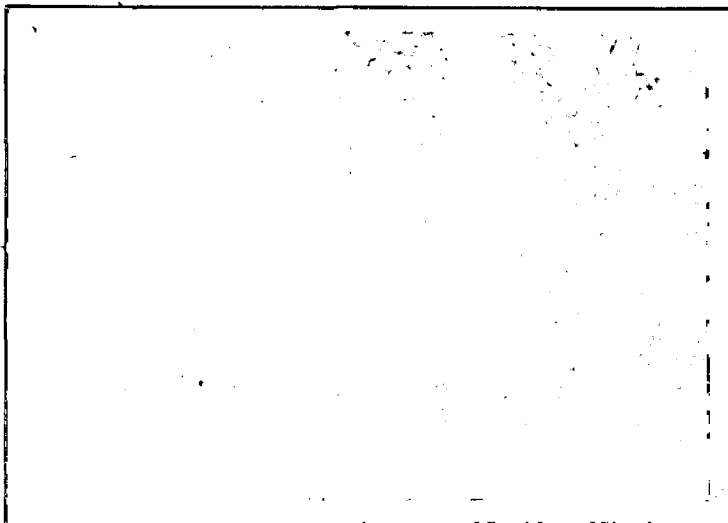


Preheat 250° C

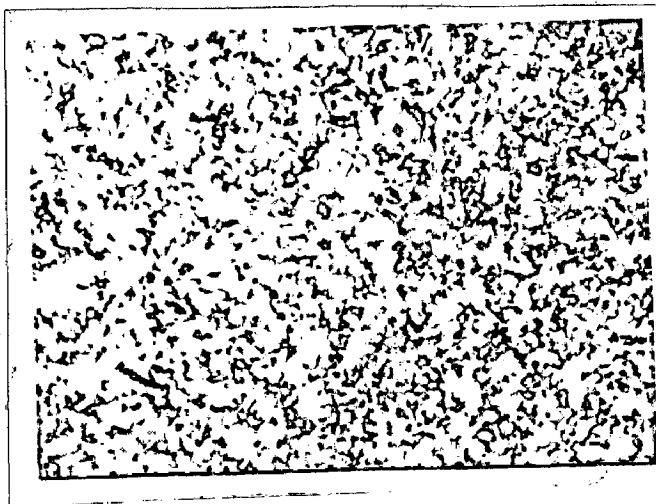
4.8(a,b,c) Micrographs at 200X showing the effect of preheating on HAZ microstructures at a PWHT of 510° C for 5 hrs using Ø3.15 mm electrodes



Preheat 100° C



Preheat 150° C



Preheat 250° C

4.9(a,b,c) Micrographs at 200X showing the effect of preheating on HAZ microstructures at a PWHT of 510° C for 10 hrs using Ø3.15 mm electrodes

TABLE 4.2 RESULTS OF MEASUREMENT OF WIDTH OF HAZ

| SPECIMEN NO. | MEAN WIDTH OF HAZ (mm) | STANDARD DEVIATION |
|--------------|------------------------|--------------------|
| D1 | 2.04 | 0.244 |
| D2 | 1.97 | 0.260 |
| E1 | 2.76 | 0.151 |
| E2 | 2.58 | 0.210 |
| F1 | 3.23 | 0.159 |
| F2 | 3.08 | 0.169 |
| A1 | 3.50 | 0.354 |
| A2 | 3.47 | 0.200 |
| B1 | 4.75 | 0.377 |
| B2 | 5.00 | 0.304 |
| C1 | 5.25 | 0.261 |
| C2 | 5.50 | 0.321 |

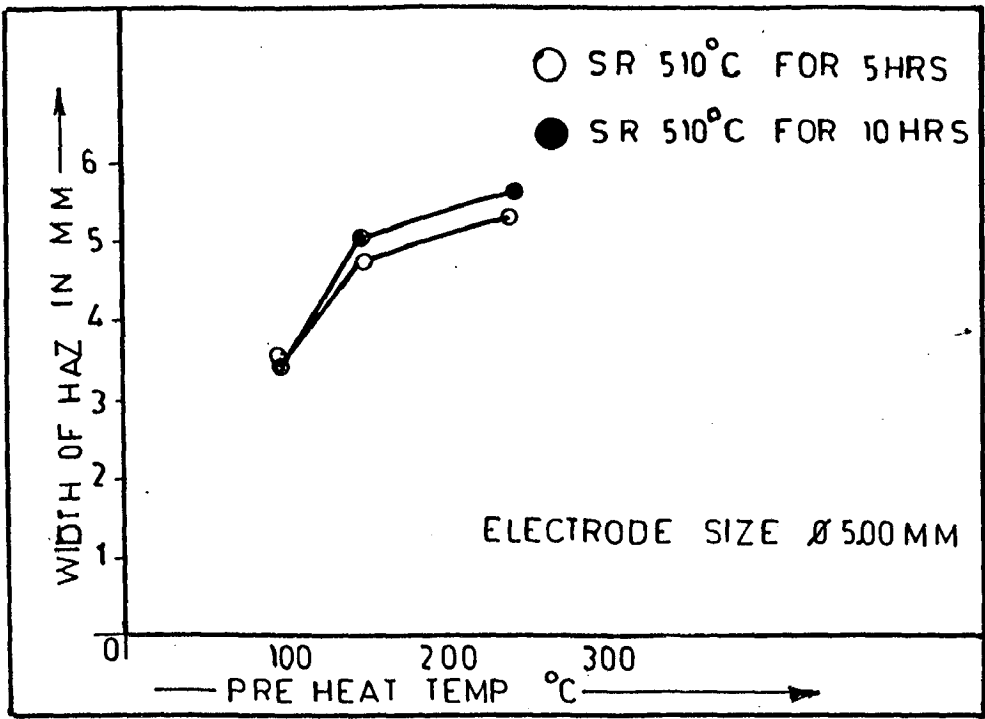


FIG 4.6 EFFECT OF PREHEAT TEMPERATURE ON THE WIDTH OF HAZ

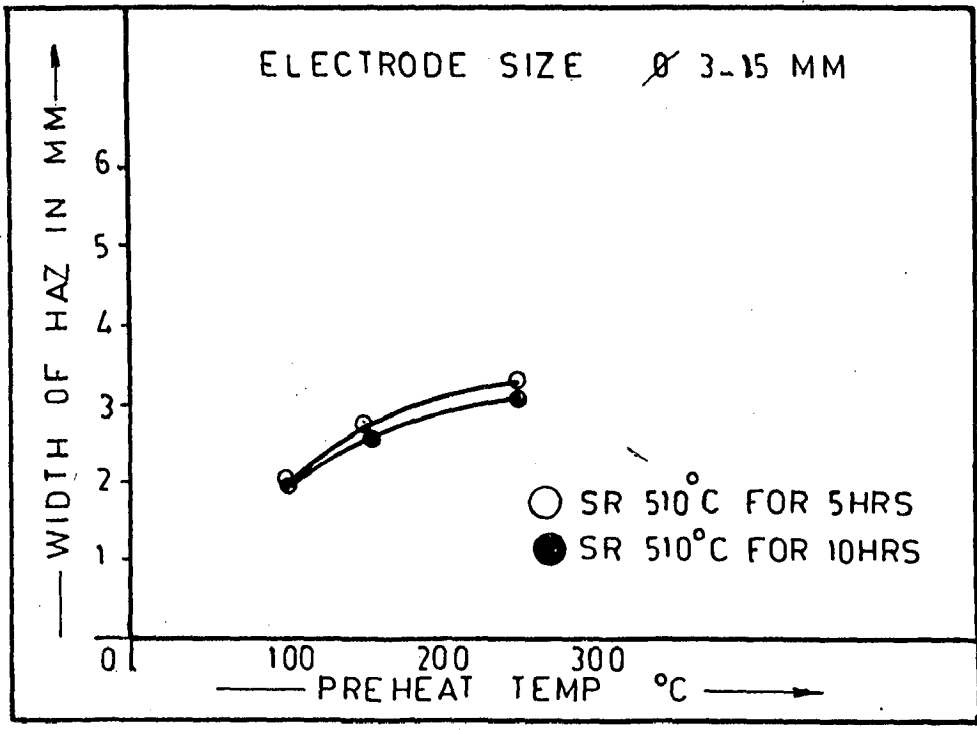


FIG 4.7 EFFECT OF PREHEAT TEMPERATURE ON THE WIDTH OF HAZ

heat treatment for 5 and 10 hrs at 510 °C on the microstructures of HAZ at a distance of 1 mm from fusion line under the different preheating conditions i.e, 100, 150 and 250 °C are shown in figs. 4.8(a,b,c) & figs 4.9(a,b,c) respectively. Similarly for electrode diameter 5.00 mm the effect of post weld heat treatment for 5 and 10 hrs at 510 °C on the microstructure of HAZ at a distance of 1 mm from fusion line under three different preheating temperatures i.e, 100, 150, and 250 °C are shown in figs. 4.10(a,b,c) and 4.11(a,b,c) respectively.

The micrographs of HAZ presented in figs. 4.8 to 4.11 show a relative grain coarsening with the increase in preheating temperature and duration of post weld heat treatment at 510 °C. However in case of welding with a low preheating temperature of 100 °C in combination with small size of electrode of 03.15 mm the HAZ was found to have microstructure consisting of martensite/bainite.

The comparatively less grain coarsening of HAZ at lower preheating of 100 °C is primarily caused by the presence of higher amount of martensite in HAZ under this condition of welding due to higher cooling rates. In case of welding using 03.15 mm electrodes especially at a low preheating of 100°C the HAZ has been found to have a significant amount of martensite/bainite transformation because of higher cooling rates prevailing at HAZ in presence of low heat input.

4.4 HARDNESS OF HAZ

Hardness of HAZ observed under different conditions of welding and post weld heat treatment has been shown in table 4.3. In case of welding using 03.15 mm electrodes effect of preheating temperature on hardness of HAZ under different conditions of post weld heat treatment for 5 and 10 hrs at 510°C has been shown in fig 4.12. Similarly in case of welding using

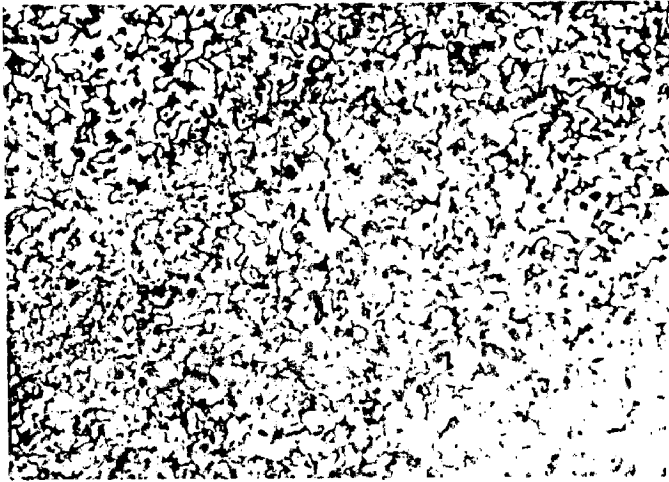
under different conditions of post welds heat treatment for 5 and 10 hrs at 510°C has been shown in fig 4.13. In both the figs. it is observed that increase in preheat temperature reduces the hardness of HAZ. The figs also show that at a given preheat temperature increase in post weld heat treatment time from 5 to 10 hrs at 510°C also marginally reduces the hardness of HAZ. But a comparison of figures 4.12 and 4.13 depicts that the use of higher diameter electrodes of $\phi 5.00$ mm comparatively enhances the hardness of HAZ with respect to that observed in case of welding with $\phi 3.15$ mm electrodes. The reduction in hardness of HAZ with increase in preheat temperature may be primarily attributed to increase in grain coarsening of HAZ during post weld heat treatment. This is possibly ~~resulted from the presence of comparatively~~ lower amount of martensite in case of higher preheating temperature, which pins down the grain coarsening.

4.5 TENSILE PROPERTIES OF WELD JOINTS

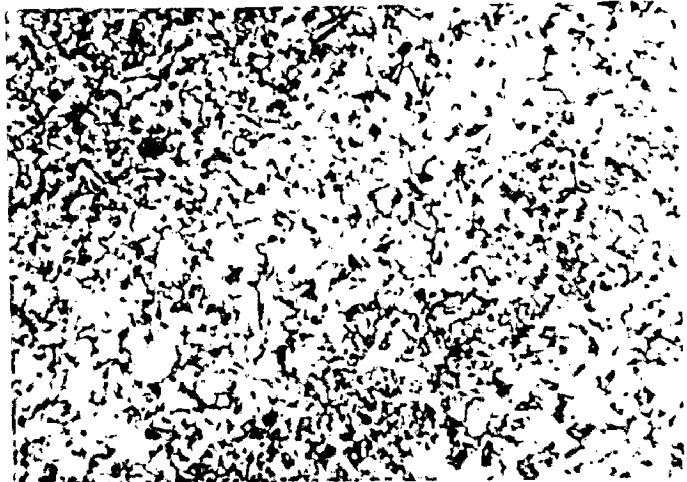
The typical behaviour of tensile load displacement curves of weld joints prepared by using $\phi 5.00$ and $\phi 3.15$ mm electrodes have been shown in fig 4.14(a & b) respectively. The curves have been shown in fig 4.14 (a & b) respectively. The curves have been found to clearly reveal the yield point of the material. During tensile test it was observed that weld joints produced by using $\phi 3.15$ mm electrodes were mostly found to fracture from weld centre (ref. fig 4.14b), whereas the weld joints prepared using $\phi 5.00$ mm electrodes always fractured from base metal, fig 4.14a. Thus it may be assumed that the yield point revealed in the curves shown in fig 4.14a represent the yield point of base material, but the yield point revealed in curves presented in fig 4.14b is represented by the yield point of weld deposit. The yield strength of the weld deposit has been marked under fig 4.14(b) as about 418.3 N/mm².



Preheat 100° C



Preheat 150° C

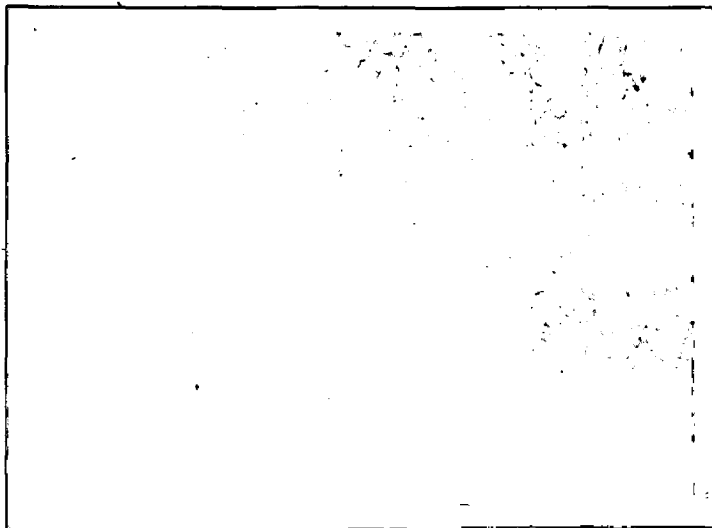


Preheat 250° C

4.8(a,b,c) Micrographs at 200X showing the effect of preheating on HAZ microstructures at a PWHT of 510° C for 5 hrs using Ø3.15 mm electrodes



Preheat 100° C

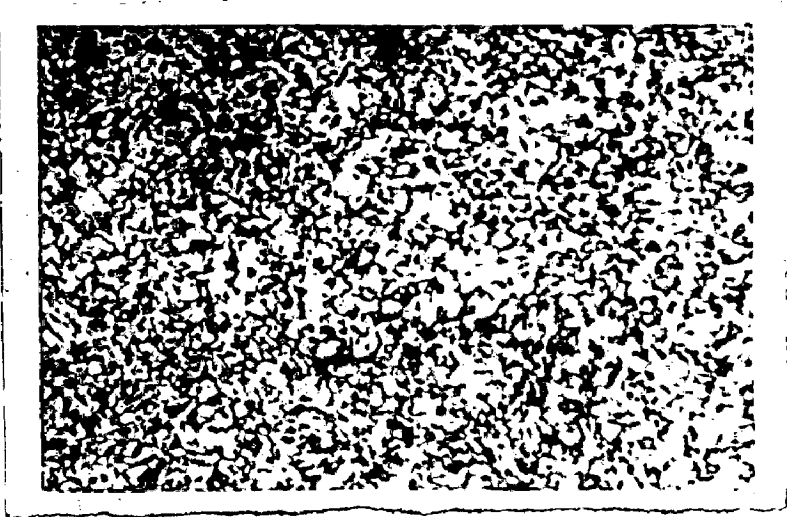


Preheat 150° C

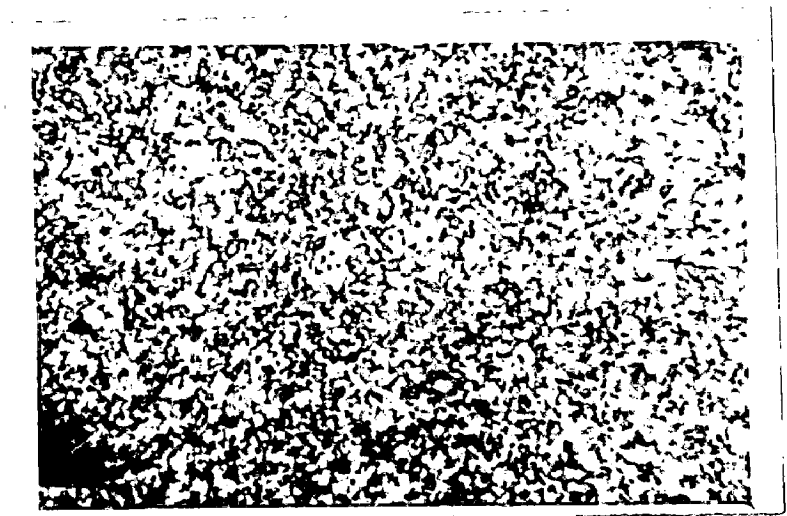


Preheat 250° C

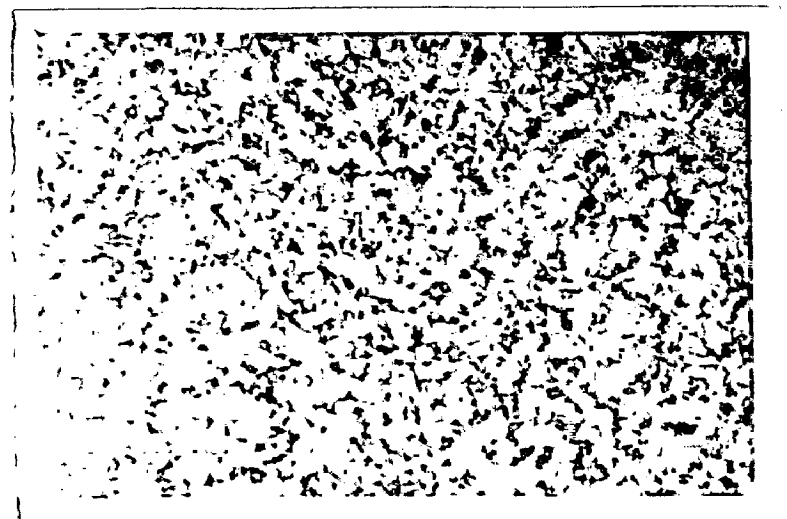
4.9(a,b,c) Micrographs at 200X showing the effect of preheating on HAZ microstructures at a PWHT of 510°C for 10 hrs using Ø3.15 mm electrodes



Preheat 100° C



Preheat 150° C



Preheat 250° C

.10(a,b,c) Micrographs at 200X showing the effect of preheating on HAZ microstructures at a PWHT of 510° C for 5 hrs using Ø5.00 mm electrodes



Preheat 100° C



Preheat 150° C



Preheat 250° C

**TABLE 4.3 : RESULTS OF MEASUREMENT OF HARDNESS AT HAZ
(HV5)**

| SPECIMEN NO. | MEAN HARDNESS (VHN) | STANDARD DEVIATION (مقياس الانحراف المعياري) |
|--------------|------------------------|--|
| D1 | 247 | 8.86 |
| D2 | 232 | 10.46 |
| E1 | 223 | 11.62 |
| E2 | 218 | 13.74 |
| F1 | 210 | 15.92 |
| F2 | 200 | 5.37 |
| A1 | 268 | 18.84 |
| A2 | 255 | 11.46 |
| B1 | 245 | 19.85 |
| B2 | 236 | 13.16 |
| C1 | 223 | 21.39 |
| C2 | 211 | 16.52 |

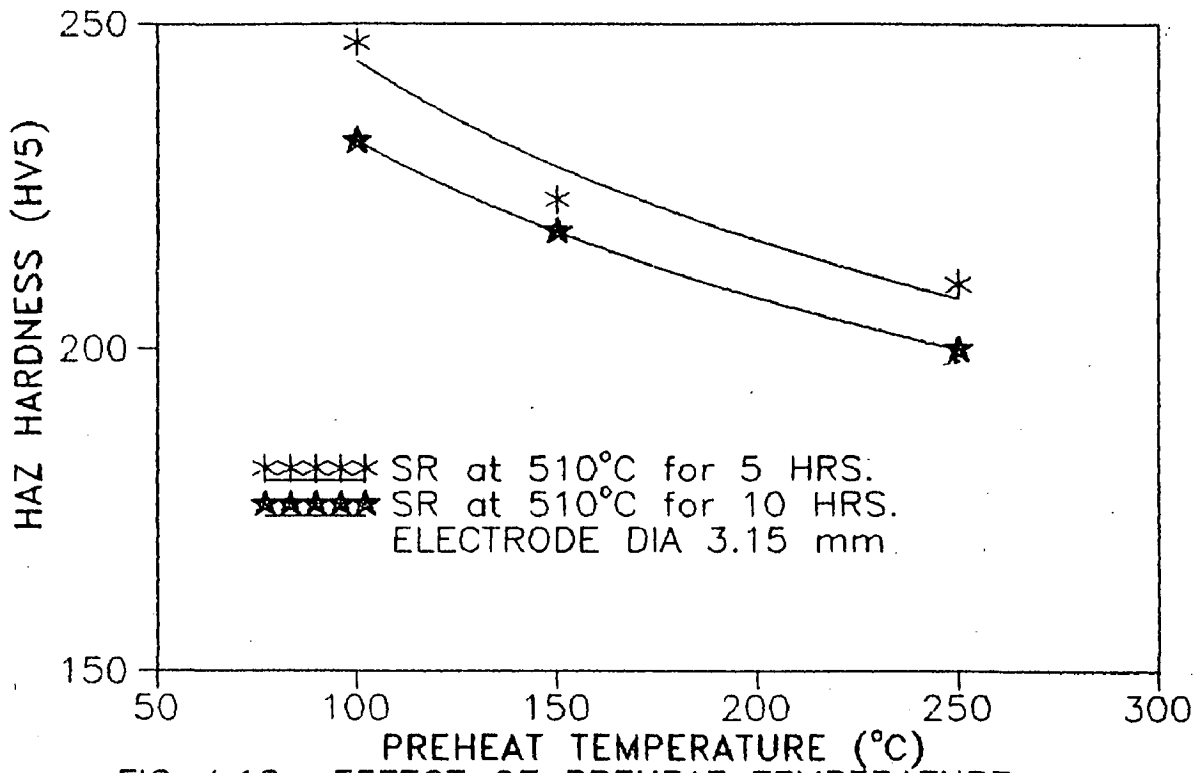


FIG 4.12 EFFECT OF PREHEAT TEMPERATURE ON HAZ HARDNESS

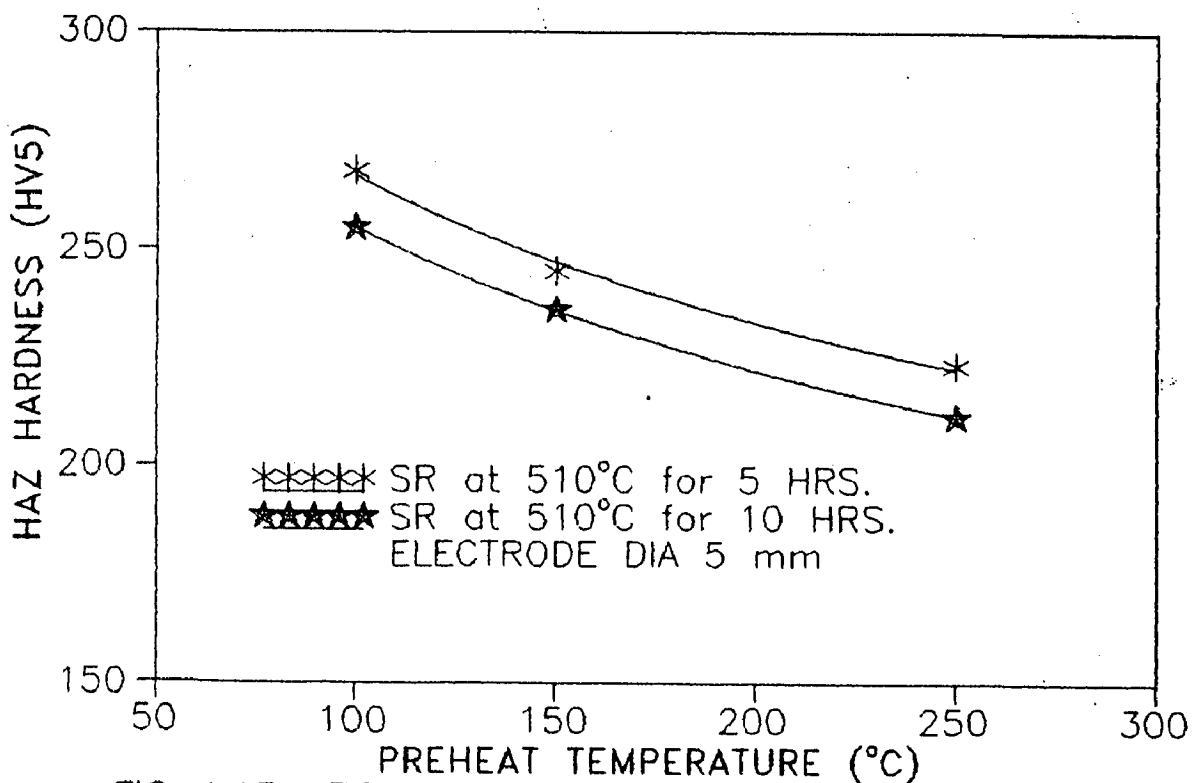


FIG 4.13 EFFECT OF PREHEAT TEMPERATURE ON HAZ HARDNESS

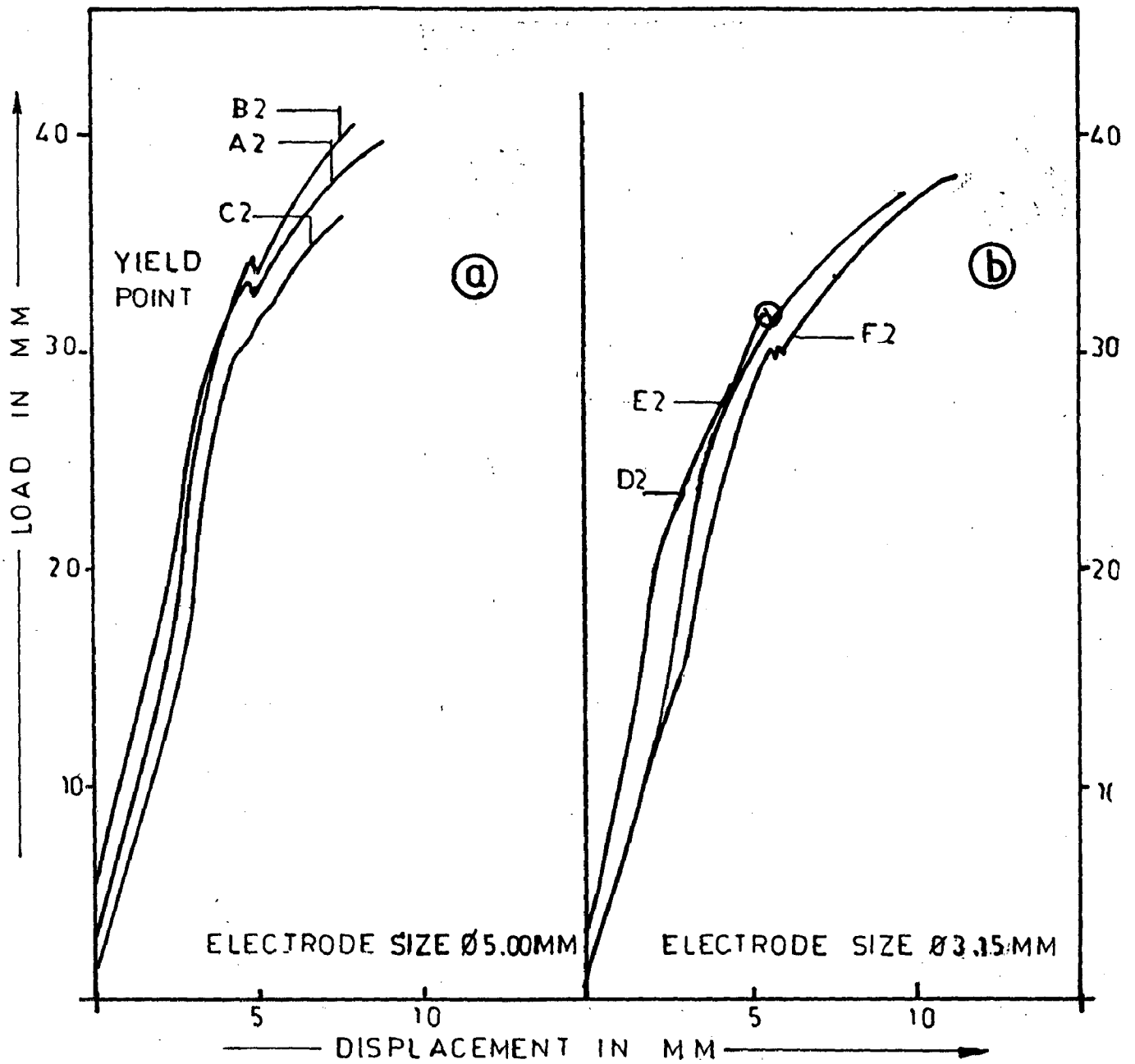


FIG.14. TYPICAL TENSILE LOAD DISPLACEMENT BEHAVIOUR OF WELD JOINT

The effect of preheat temperature on ultimate tensile strength of weld joints in case of post weld heat treatments of 5 and 10 hrs at 510°C has been shown in fig 4.15 when the electrode of 3.15 mm dia was used. Similarly the effect of preheat temperature on ultimate tensile strength of weld joints under post weld heat treatment of 5 and 10 hrs at 510°C has been shown in fig 4.16 when a higher diameter electrode of 5.00 mm was used. Fig 4.15 shows that during the use of given size of electrode of 3.15 mm the increase in preheating temperature as well as the duration of post weld heat treatment significantly reduces the ultimate tensile strength of the weld deposit, when it is fractured from weld metal. This may be attributed to increase in grain coarsening of weld deposit as it has been discussed to earlier with reference to their microstructures. However the observed decrease in strength of weld joints fractured from base material, with the increase in preheat temperature may be primarily attributed to reduction in residual stresses of the base material resulted from forging operation of the shaft.

4.6 FATIGUE PROPERTIES OF WELD JOINTS

In case of welding using $\phi 3.15$ mm electrodes, the effect of preheat temperature and duration of post weld heat treatment on fatigue life of weld joints has been shown in fig 4.17. Similarly in case of welding using higher diameter electrode of 5.00 mm, the effect of preheating and duration of post weld heat treatment on fatigue life of weld joints has been shown in figure 4.18. During the fatigue testing of weld joints, the specimens are always found to fracture from base material. Thus the results presented in figures 4.17 and 4.18 do not represent the fatigue properties of weld joints. The observed trend of lowering the fatigue life of weld joints, fractured from base material with the increase in preheat temperature as well as duration of post weld heat treatment may be primarily happened due to lowering of tensile strength of base material as discussed earlier. However the fatigue

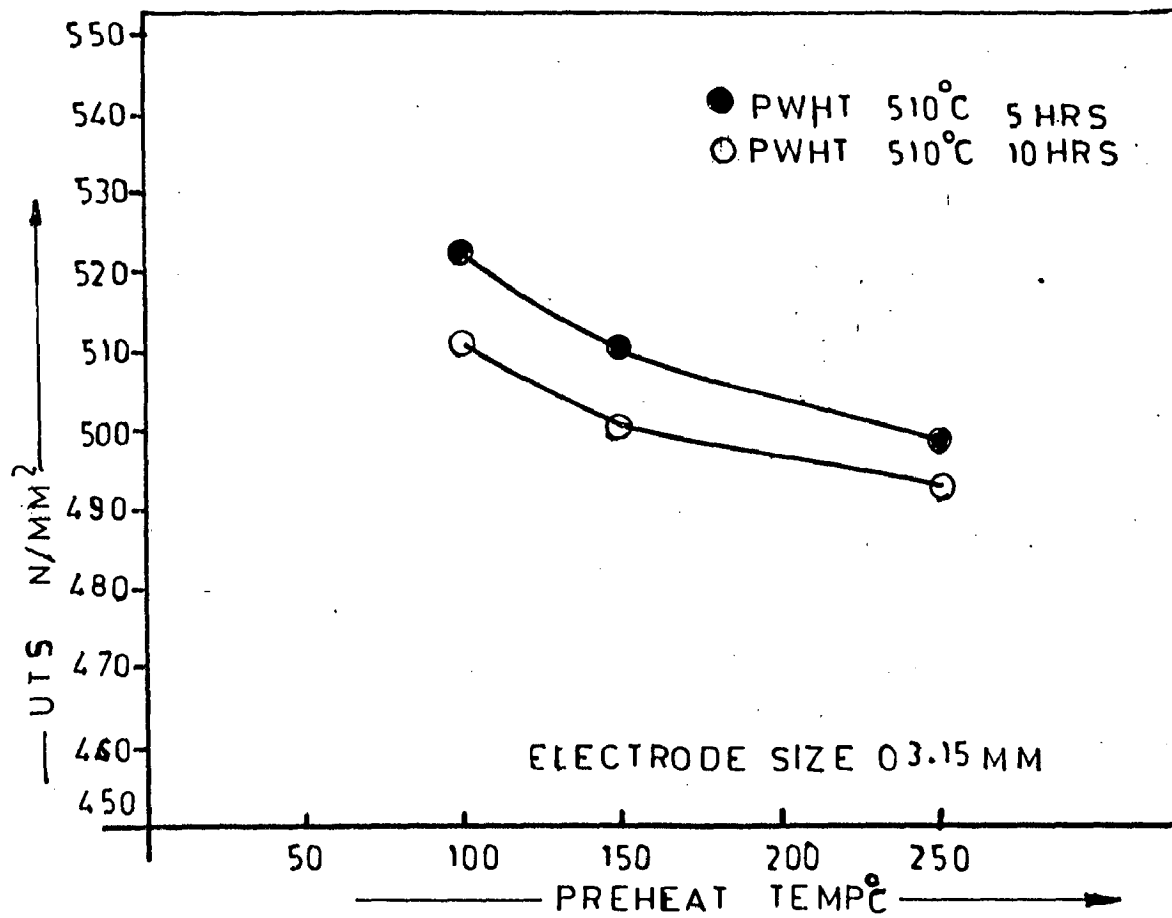


FIG 4.15 EFFECT OF PREHEAT TEMPERATURE AND DURATION OF PWHT ON UTS OF WELD JOINTS

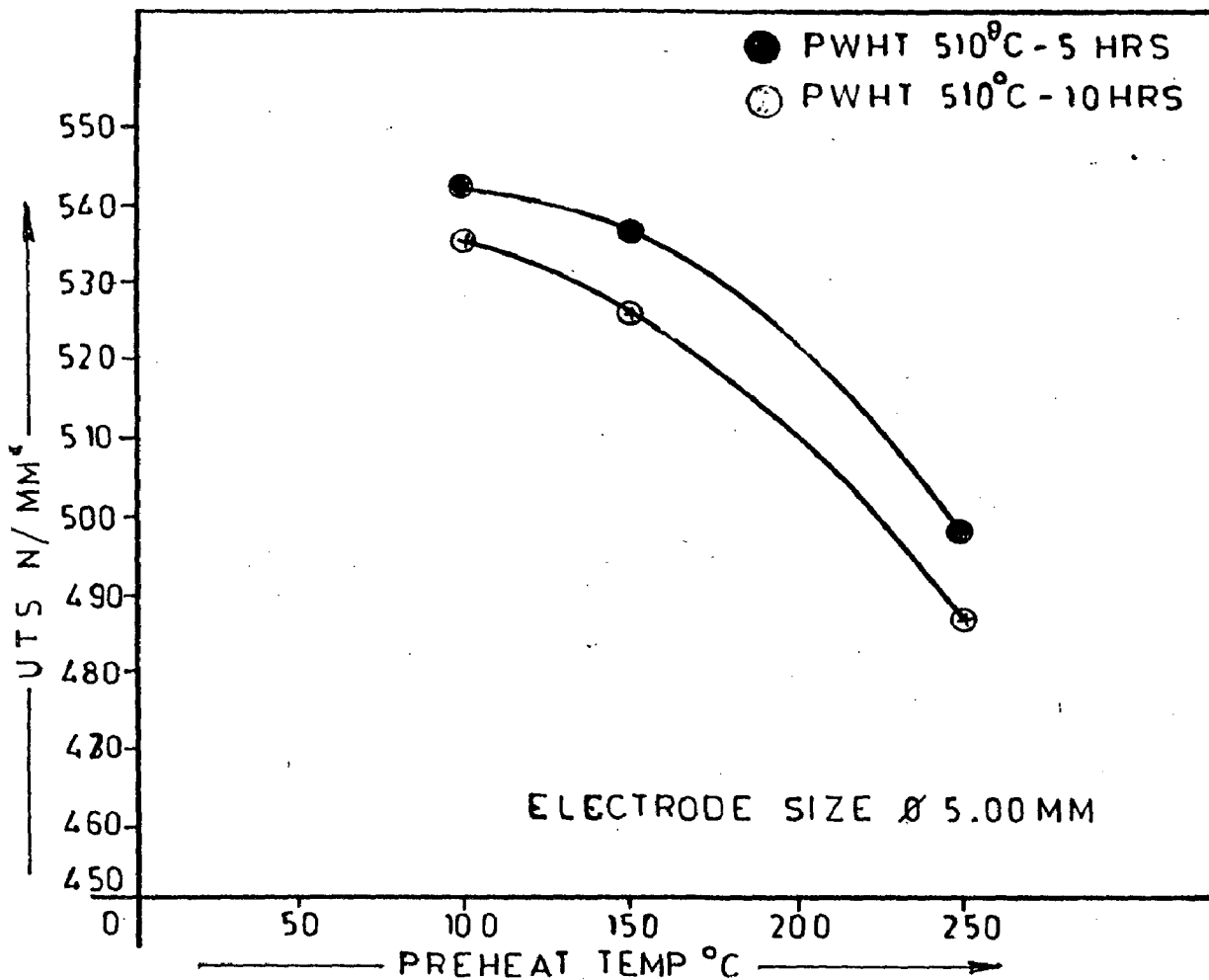


FIG 4.16 EFFECT OF PREHEAT TEMP AND DURATION OF PWHT ON UTS OF WELD JOINTS

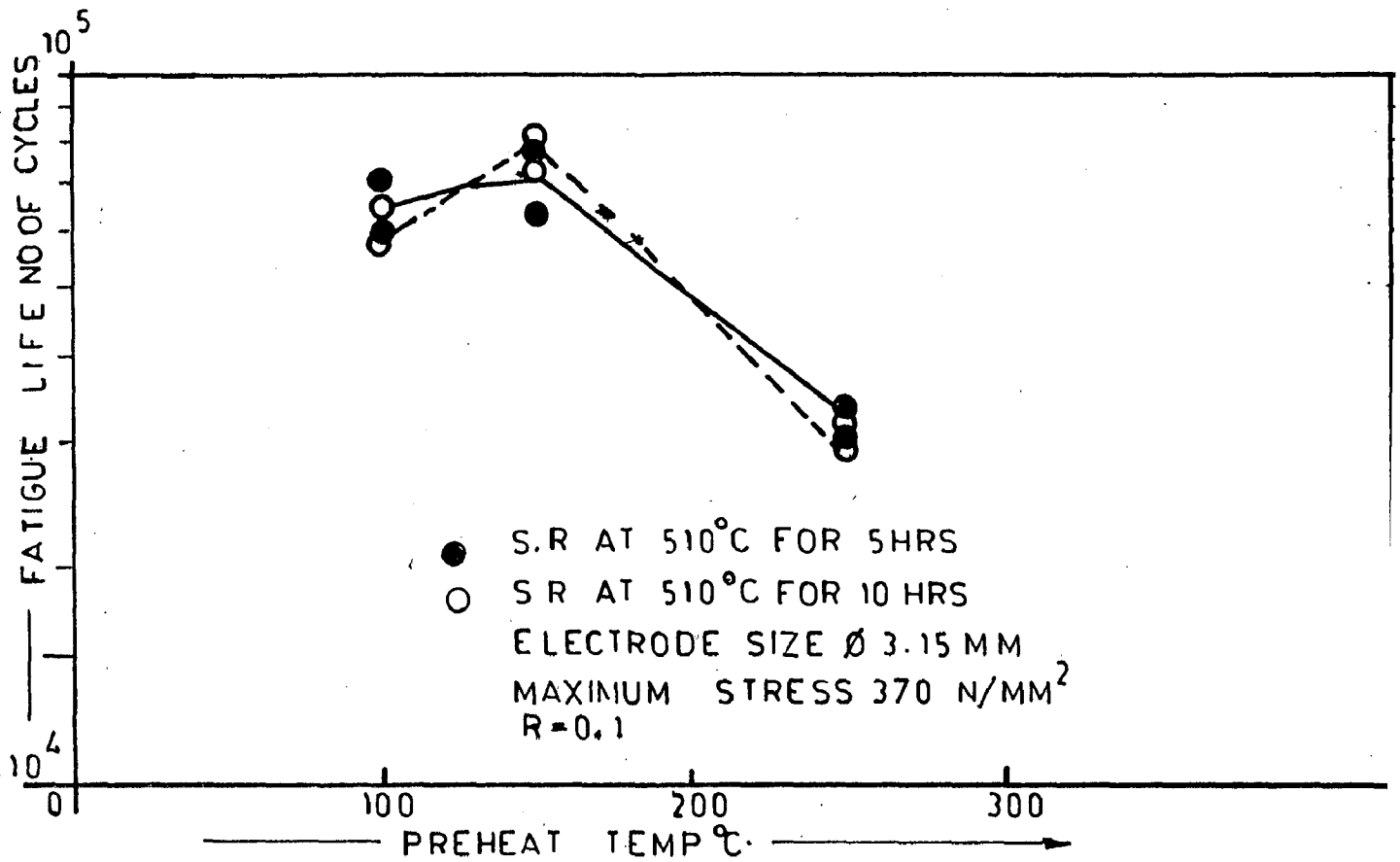


FIG 4.17 EFFECT OF PREHEAT TEMP AND DURATION OF PWHT ON FATIGUE LIFE OF WELD JOINT

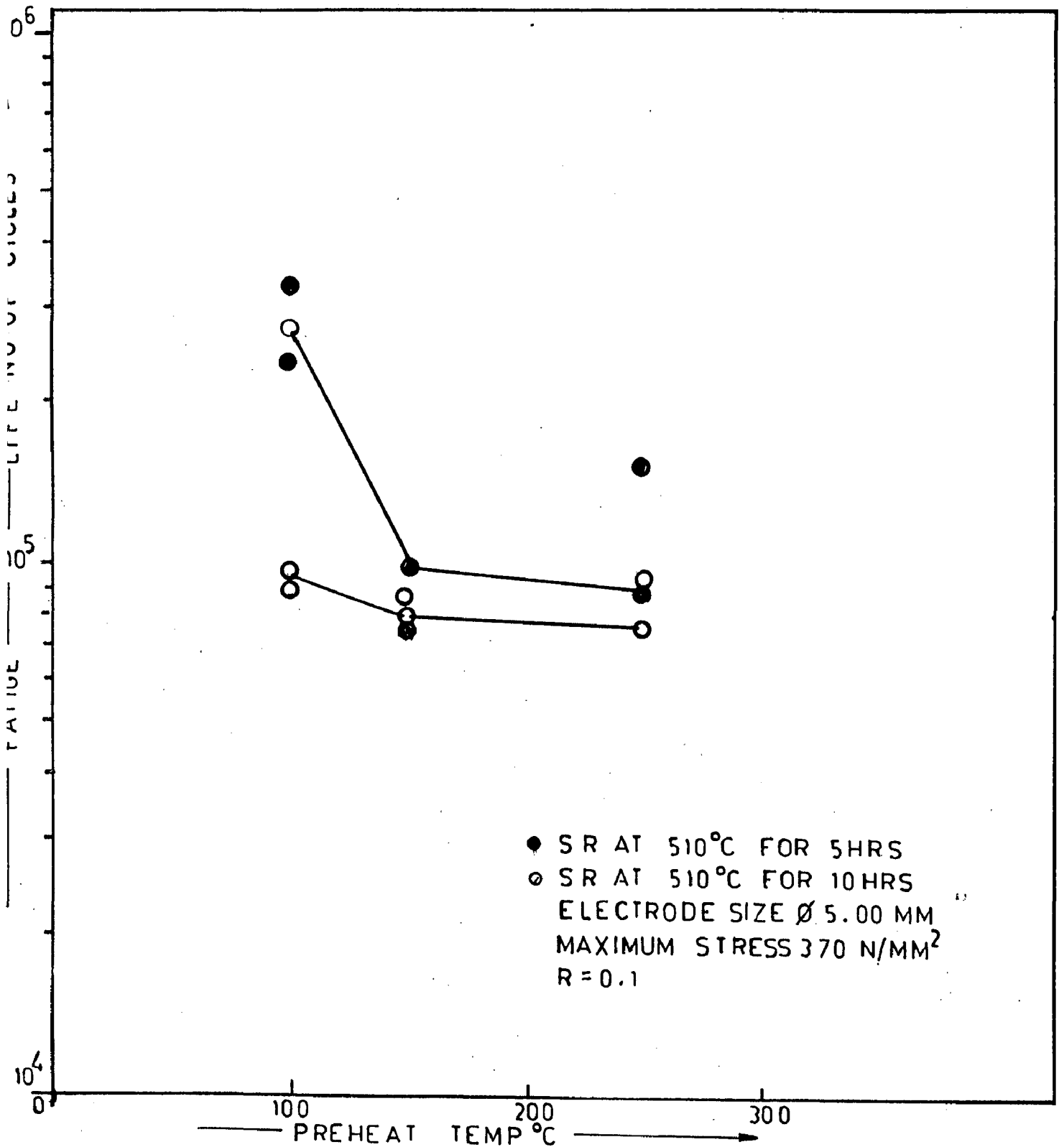


FIG 4.18 EFFECT OF PREHEAT TEMP AND DURATION OF PWHT ON FATIGUE LIFE OF WELD JOINTS

TABLE 4.4

RESULTS OF FATIGUE TEST CARRIED OUT ON WELDED SPECIMEN AT
 MAXIMUM STRESS 370 N/mm² AND R = 0.1

| SPECIMEN No. | CROSS-SECTIONAL AREA (mm ²) | CYCLES TO FAILURE |
|--------------|--|----------------------|
| A1 | 78.5 | 1,32,700 |
| | 81.67 | 1,24,450 |
| B1 | 80.07 | 74,470 |
| | 78.50 | 97,320 |
| C1 | 80.07 | 1,10,500 |
| | 81.67 | 89,900 |
| A2 | 78.50 | 93,390 |
| | 78.50 | 89,000 |
| B2 | 80.07 | 87,000 |
| | 78.50 | 79,490 |
| C2 | 78.50 | 76,580 |
| | 78.50 | 89,000 |
| D1 | 78.50 | 70,300 |
| | 80.07 | 60,500 |
| E1 | 78.50 | 62,800 |
| | 78.50 | 79,400 |
| F1 | 78.50 | 35,900 |
| | 78.50 | 34,000 |
| D2 | 81.67 | 66,000 |
| | 78.50 | 59,000 |
| E2 | 81.67 | 81,000 |
| | 78.50 | 76,540 |
| F2 | 80.07 | 32,000 |
| | 78.50 | 30,150 |

CHAPTER-5

CONCLUSION

1. Increasing the preheat temperature from 100°C to 250°C and electrode size from ϕ 3.15 to ϕ 5.00 mm enhances the coarsening of grain size and peralite colonies in the weld deposit during post weld heat treatment.
2. Use of low preheating temperatures and smaller diameter of electrodes reduces grain coarsening of heat zone during post weld heat treatment due to promotion of martensite transformation.
3. Fatigue life of welds is superior to that of base metal under the present conditions of welding used in this investigations i.e, preheating from 100 to 250°C, electrode size ϕ 3.15 to 5.00 mm and 5 to 10 hrs duration of post weld heat treatment of 510°C.
4. During the use of higher diameter of electrode of 5.00 mm, weld metal is superior to base metal under tensile test of weld joints.
5. It is recommended to carry out repair of shaft forging to C-Mn steels using following parameters:
 - a.
 - i) Electrode size ϕ 3.15 mm
 - ii) Preheat temperature 150°C
 - iii) PWHT-5 hrs at 510°C
 - b.
 - i) Electrode size ϕ 5.00 mm
 - ii) Preheat temperature 100°C
 - iii) PWHT-5 hrs at 510°C

SCOPE FOR FUTURE WORK

It is recommended that the effect of various welding parameters on mechanical and fatigue properties of repair welds of forgings should be carried out further by collecting specimens from all weld metal, as well as from the specific region of heat affected zone.

LIST OF REFERENCES

1. Defects in ingots and their products, Special report No 63, The Iron and Steel Institute London pp 25-43.
2. C. MACCOCAIRE : " Repair welding : How to set up a shop."
Welding Journal August 1991 pp 54-56.
3. V. Malin and S.F. Fields., "A balanced approach to repair of large structures by Welding", Welding Journal, March 1992 pp 63-72.
4. Lancaster J.F. "Metallurgy of Welding", Metallurgical effects of the weld thermal cycles, chapter 4.0 pp 53-93 Fourth ed.
1987.
5. Tremlett, H.F. "Welding manual for engineering steel forgings", part 1, "Fusion Welding of Carbon and alloy engineering steel forgings" pp 1-44. Pentech press Ltd. 1976, London.
6. Davin Yosh and Alexander Caploon : "Successful welding repair of turbine casing cracks", Welding Journal, February 1992, pp 29-35.
7. T.A. Sievert, R.P. Reep, D.A. Shepherd and S.P. Sobczynski, "Weld cracking in Massive steel forgings", Welding journal Oct 1989 pp 23-30.

8. **Richard B. Corbit and Stephen M. French, "Weld repair adds life to power plant turbine", Welding Journal, Jan 1997, pp 51-55.**
9. Dr.(Ing) Tadeusz Robakowski, "Investigations into the fatigue life of shafts surfaced by welding", Schweissen Schneiden 6/92.
10. Dr. P. K. Ghosh, "Failure investigations in weldment." 1988,
E 1.10/633.98
11. "Common Thermal treatments for weldments", Welding hand book Sixth ed. pp 5.23-5.37.
12. "A mathematical investigation of the local stress relief heat treatment of repair welds and procedural guidelines", Schweissen Schneiden 9/87.
13. **"Weldment Distortion", Procedure Hand Book of Arc Welding", The Lincoln Electric Co. Cleveland Ohio 12th ed, pp 3.1-4 - 3.1-19.**